國立臺灣大學生命科學院分子與細胞生物學研究所

碩士論文

Institute of Molecular and Cellular Biology
College of Life Science
National Taiwan University

Master Thesis

以斑馬魚 *nicastrin* 基因異型合子突變種為神經退化模型之研究

Neurodegeneration Study On Zebrafish *nicastrin* Heterozygous Mutants

陳文傑

Wen-Jie Chen

指導教授：江運金 博士

Advisor: Yun-Jin Jiang, Ph.D.

中華民國 107 年 8 月

August 2018

doi:10.6342/NTU201803306

致謝

這是我第一次長時間待在一間實驗室裡做研究；一開始什麼都不懂，先學習自己在網路上，找和研究題目相關的論文閱讀，吸收相關領域的知識；接著學習各式各樣的實驗方法，從剪尾巴抽基因組 DNA、取腦抽 RNA 和蛋白質、進行斑馬魚行為測試到做冷凍切片及免疫染色，慢慢能獨自完成一個又一個的實驗；接下來還要學習如何解決實驗上遇到的問題，透過和別人討論，聽取他人的經驗以及在網路上搜尋相關資料，去找出實驗結果不理想的原因；最後要學習如何分析實驗結果，並運用自己的知識及網路上的資料庫去解釋結果，做出結論並發想下一次的實驗。這條路雖然辛苦，卻也很值得。

一路走來，要感謝許多人。特別要感謝的是我的指導教授—江運金老師，讓我進入這個實驗室，讓我有機會在這裡學習，做我有興趣的研究；還要感謝負責管理斑馬魚核心實驗室的游美淑老師，時常給我實驗上的建議及鼓勵；感謝實驗室的同仁，在我遇到實驗上的問題時能夠幫助我找出問題並且加以解決－感謝家豪學長教我許多做實驗的方法及分享好用的免費軟體；感謝莉娟學姊教我做西方墨點法以及做 construct，協助我在 HEK293T 細胞過量表現目標蛋白，並且在實驗上給予我許多建議；感謝國彰學長教我如何取斑馬魚的腦，並和我討論實驗結果；感謝健銘學長教我做行為實驗；感謝已經成為助理教授的議賢學長，離開實驗室之後讓我不停打擾問問題；感謝後來加入實驗室的大瑋學長，給予我研究上的建議，並且和我討論實驗上的作法；感謝美香姊把斑馬魚照顧得很好，並且會不時地提供食物。感謝威凱學長找我一起打籃球，讓我偶爾能活動一下筋骨；也很感謝、潔怡、羽萱、以倢和亞晴營造實驗室的歡樂氣氛。我還要感謝兩位口試委員－管永恕老師以及黃筱鈞老師，在口試時點出問題並給我許多建議。最後，要感謝我的家人，在背後給我支持，並且包容我這麼長時間都不回家。我要畢業了，要往下個階段邁進。謝謝大家。祝大家身體安康，快快樂樂。

doi:10.6342/NTU201803306

中文摘要

目前已知伽馬分泌酶 (γ-secretase)在神經退化疾病中扮演重要角色，而 Nicastrin 是伽馬分泌酶其中一個次單元，其功能為調控伽馬分泌酶與受質的結合。先前研究報導指出在老鼠神經細胞條件式敲除 *nicastrin* 基因會導致神經退化，然而其機制尚不清楚。我們實驗室先前也在一個異型合子 *nicastrin* 基因突變 (*nicastrin*$^{hi1384/+}$) 斑馬魚中發現神經退化的症狀，包括高度磷酸化 Tau 蛋白增加以及認知能力下降。因此我們希望全盤檢測分析此種斑馬魚的神經退化症狀，並評估其是否能成為神經退化研究的模式生物。我們使用斑馬魚行為軌跡追蹤系統探討 *nicastrin*$^{hi1384/+}$斑馬魚幼魚行為，發現其在光照刺激期間相較同齡野生種 (wild type) 斑馬魚幼魚有更高的活動力。另一方面，使用 T 型迷宮行為試驗檢測此 *nicastrin*$^{hi1384/+}$斑馬魚成魚的認知能力，在排除運動能力差異的影響後，初步結果顯示年齡為 12 個月及 18 個月的 *nicastrin*$^{hi1384/+}$斑馬魚，其認知能力明顯變得比同齡野生種 (wild type) 斑馬魚還要低。然而由於先前在行為實驗中使用的食物被用盡且無法再取得，我們更換了行為實驗中的食物，後續的實驗無法完全重複上述行為實驗結果，但 18 個月的 *nicastrin*$^{hi1384/+}$斑馬魚認知能力依然有較差的趨勢。此外，使用基因微陣列分析 T 型迷宮行為試驗受試班馬魚腦中的轉錄組 (transcriptome)，結果顯示在 *nicastrin*$^{hi1384/+}$斑馬魚腦中 *nicastrin* 訊息 RNA 的表現量下降，而其餘伽馬分泌酶次單元的訊息 RNA 表現量並不受影響。上述結果皆在即時聚合酶鏈鎖反應 (quantitative real-time PCR, qPCR) 實驗中得到證實。最後，運用轉錄組功能分析基因微陣列的數據，結果預測在轉錄層級上年長的 *nicastrin*$^{hi1384/+}$斑馬魚腦中，神經退化症狀受到促進，另一方面，神經存活、神經分化及神經功能的維持受到抑制，說明年長的 *nicastrin*$^{hi1384/+}$斑馬魚的腦在轉錄的層級上有神經退化的現象。然而使用末端脫氧核苷酸轉移酶脫氧尿苷三磷酸切口末端標記 (Terminal deoxynucleotidyl transferase dUTP nick end labeling, TUNEL) 檢測腦中細胞凋亡情

doi:10.6342/NTU201803306

形，結果顯示 18 個月的 *nicastrin*$^{hi1384/+}$與同齡野生種組別並無差異，未來有必要使用其他神經退化的生物標誌來檢測 *nicastrin*$^{hi1384/+}$斑馬魚的腦中是否出現神經退化的症狀。

總結來說，*nicastrin*$^{hi1384/+}$斑馬魚幼魚在光照環境下相較於野生種斑馬魚幼魚有較高的活動力，表示 *nicastrin*$^{hi1384/+}$斑馬魚與野生種斑馬魚在神經迴路發育過程中可能有些差異。另一方面，我們證實了在 *nicastrin*$^{hi1384/+}$斑馬魚腦中，*nicastrin* 訊息 RNA 表現量下降。再者，行為實驗及轉錄組分析結果皆顯示年長 *nicastrin*$^{hi1384/+}$斑馬魚有神經退化的趨勢。上述結果顯示 *nicastrin*$^{hi1384/+}$斑馬魚具有做為神經退化動物模型的潛力。未來我們需要在年長的 *nicastrin*$^{hi1384/+}$斑馬魚的腦中檢視其他神經退化症狀，例如神經發炎反應、神經細胞數量減少、神經萎縮及突觸減少等等。

doi:10.6342/NTU201803306

Abstract

Nicastrin is a subunit of γ-secretase which functions to regulate binding of substrates to γ-secretase and has been implicated in neurodegeneration. However, the mechanism is unclear. Previously, we discovered several neurodegenerative phenotypes, including increased hyperphosphorylated Tau proteins and cognition deficits in aged *nicastrin*$^{hi1384/+}$ zebrafish (unpublished data). Accordingly, we intended to comprehensively examine if *nicastrin*$^{hi1384/+}$ zebrafish can be a vertebrate model to study neurodegeneration. In the present work, we conducted a visual motor response test on *nicastrin*$^{hi1384/+}$ zebrafish larva and uncovered that they were more active under light stimulus than wild type zebrafish larva. Besides, original T-maze behavioral tests on *nicastrin*$^{hi1384/+}$ zebrafish demonstrated that memory of 12 and 18 month *nicastrin*$^{hi1384/+}$ zebrafish were impaired compared to wild type zebrafish at the same age after excluding the influence of mobility variation. However, as the food which had been used in the previous behavioral tests was run out and unavailable, we switched to a new kind of food and failed to recapitulate the original behavioral tests results in the latter behavioral tests. Nevertheless, memory of *nicastrin*$^{hi1384/+}$ zebrafish was still worse than wild type at 18 month of age. On the other hand, transcriptomic analysis on the brains of subject zebrafish of behavioral tests by using microarray showed that *nicastrin* mRNA level was

doi:10.6342/NTU201803306

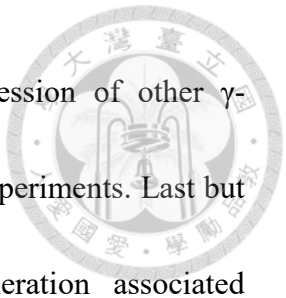

downregulated in *nicastrin*$^{hi1384/+}$ zebrafish, whereas mRNA expression of other γ-secretase subunits was not affected, which were verified by qPCR experiments. Last but not least, disease and functional analysis showed neurodegeneration associated phenotypes were activated, while neuronal survival and functions associated phenotypes were inhibited, implicating that *nicastrin*$^{hi1384/+}$ zebrafish have age-dependent neurodegeneration at transcriptional level. However, TUNEL staining displayed no extensive neuronal apoptosis in the telecephalon of 18 month *nicastrin*$^{hi1384/+}$ zebrafish.

In conclusion, *nicastrin*$^{hi1384/+}$ zebrafish larva displayed higher activity than wild type under light stimulus, and the mechanism needs to be further clarified. On the other hand, we verified the expression of *nicastrin* was reduced in the brains of adult *nicastrin*$^{hi1384/+}$ zebrafish by both microarray and qPCR. Furthermore, both behavioral and transcriptomic analysis demonstrated the trend of age-dependent neurodegeneration in *nicastrin*$^{hi1384/+}$ zebrafish, suggesting that *nicastrin*$^{hi1384/+}$ zebrafish have potential to be a neurodegeneration model. In the future, we should examine other neurodegeneration phenotypes, such as neuroinflammation, neuronal loss, neuritic dystrophy, and synaptic loss in the brains of aged *nicastrin*$^{hi1384/+}$ zebrafish.

doi:10.6342/NTU201803306

Table of Contents

doi:10.6342/NTU201803306

Index of Figures

Index of Tables

Index of Supplementary Figures

doi:10.6342/NTU201803306

Chapter 1. Introductions

1.1 Introduction to Alzheimer's Disease

Alzheimer's disease which was firstly described by a German psychiatrist, Alois Alzheimer in 1907 is the most prevailing neurodegenerative disease. The symptoms of Alzheimer's disease include brain atrophy, extensive distribution of neuronal tangles and amyloid plaques, astrogliosis, neuronal dystrophy, neuronal loss and vascular alterations (De Strooper and Karran, 2016). Patients with Alzheimer's disease suffer from emotional alterations and cognitive impairments, accordingly loss of self-care abilities. Eventually, Alzheimer's disease leads to death. Taking care of Alzheimer's disease patients has become a huge mental and financial burden on society, particularly when the population is aging (Prince, 2016). Unfortunately, despite tons of efforts have been made, the etiology of Alzheimer's disease is still ambiguous. Accordingly, diagnosing Alzheimer's disease in the early stage is difficult and there is no efficient treatment for Alzheimer's disease. As a result, delineating the mechanisms of Alzheimer's disease is an urgent topic (Kumar et al., 2015).

The hallmarks of Alzheimer's disease are intracellular neurofibrillary tangles and extracellular amyloid plaques (Guillozet et al., 2003). Intracellular neurofibrillary tangles are made up with Tau proteins. Tau protein is a microtubule binding protein. Upon

doi:10.6342/NTU201803306

hyperphosphorylation, Tau proteins get easily detached from microtubules and tend to aggregate to form tangles inside the cells (Wang and Mandelkow, 2016). On the other hand, extracellular amyloid plaques are composed of Aβ peptides (Glenner and Wong, 1984; Masters et al., 1985). The identification of Aβ peptides led to amyloid cascade hypothesis which assumes that Aβ peptide is the culprit of Alzheimer's disease, resulting in neurofibrillary tangles formation, astrogliosis, neuronal loss, and eventually learning and memory deprivation (Hardy and Higgins, 1992; Hardy and Selkoe, 2002). Aβ peptide 'is produced from serial cleavages by β-secretase and γ-secretase on the Amyloid Precursor Protein (APP) which is a type I transmembrane protein. β-secretase cleaves APP in the extracellular domain, and subsequently γ-secretase processes APP in the transmembrane domain (Plant et al., 2003). Owing to the involvement of Aβ peptides production, γ-secretase has drawn the attention in Alzheimer's disease research and has been considered an important target for Alzheimer's disease treatment (Mitani et al., 2012; Golde et al., 2013).

1.2 Introduction to γ-secretase and Its Subunits

γ-secretase was initially used to describe the proteolytic activity that processes the Amyloid Precursor Protein (APP) in the transmembrane domain (Haass and Selkoe, 1993). Later, it was found to be a multi-subunit protease complex (De Strooper et al.,

doi:10.6342/NTU201803306

2012). γ-secretase is located on intracellular and plasma membranes, and conducts intramembrane cleavage on various type I transmembrane proteins aside from APP, such as Notch (Zhang et al., 2014; De Strooper et al., 1999). γ-secretase processing on Notch releases Notch intracellular domain (NICD) which is translocated to the nucleus, serving as a transcriptional factor to induce gene expression, and regulate developmental processes (Shih and Wang, 2007).

γ-secretase consists of four subunits, which are Presenilin, Nicastrin, APH-1 and PEN-2 (Kimberly et al., 2003). Presenilin is an aspartyl intramembrane protease and the catalytic center of γ-secretase (Wolfe et al., 1999; Esler et al., 2000). Presenilin has two isoforms in humans, Presenilin-1 and Presenilin-2. Various missense mutations on Presenilin-1 and Presenilin-2 result in production of extended Aβ peptides, Aβ42, which are more inclined to aggregate to form amyloid plaques in the brain than normal Aβ-peptides, Aβ40. These mutations are autosomal dominant and can lead to early onset familial Alzheimer's disease (FAD) (Vetrivel et al., 2006; De Strooper et al., 2012). APH-1 is essential for the assembly and activity of γ-secretase, and also a regulator of cellular localization of Nicastrin (Goutte et al., 2002; Lee et al., 2004). Pen-2 facilitates the endoproteolysis of full-length Presenilin in the loop domain between TM6 and TM7 , turning full-length Presenilin into active NTF and CTF, which is indispensable for the catalytic function of Presenilin (Zhang et al., 2014; Hasegawa et al., 2004). Nicastrin is a

doi:10.6342/NTU201803306

type I transmembrane protein which is composed of a large, highly glycosylated extracellular domain, a transmembrane domain, and a short C-terminus (Xie et al., 2014). Previous studies suggest that Nicastrin is dispensable for γ-secretase intracellular protease activity, but is crucial for intracellular transportation of γ-secretase and its stability (Zhao et al., 2010; Zhang et al., 2005). Recent studies show that the large extracellular domain of Nicastrin serves as a gatekeeper to prevent non-substrate proteins from being processed by γ-secretase, which is critical to regulate γ-secretase activity on non-substrate membrane proteins (Bolduc et al., 2016; Urban, 2016).

In addition, there are several γ-secretase independent biological functions for each γ-secretase subunit. Presenilin-1 has been documented to involve in multiple cellular processes in a γ-secretase independent manner, including Wnt/β-catenin signaling, calcium homeostasis, cellular survival and protein trafficking and degradation (Duggan and McCarthy, 2016; Zhao et al., 2017). Nicastrin was shown to affect Akt and p53-dependent pathway at the post-transcriptional level and control cell death (Pardossi-Piquard et al., 2009). APH-1 and Pen-2 were reported to lower p53-dependent control of caspase-3 and trigger an anti-apoptotic response (Dunys et al., 2007).

Both γ-secretase dependent and independent biological functions have been implicated in Alzheimer's disease and other neurodegenerative diseases (Thinakaran and Parent, 2004; Campbell et al., 2006; Katia et al., 2013; Carroll and Li, 2016). The ability

doi:10.6342/NTU201803306

of γ-secretase to process various substrates and its multifunctional subunits makes it complicated to develop treatments for neurodegeneration by simply targeting γ-secretase (Basi et al., 2010). Drugs produced under inadequate knowledge base could result in many side effects. Consequently, it's necessary to comprehensively understand the biological functions of γ-secretase subunits.

1.3 Nicastrin and Neurodegeneration

So far, Presenilin gets much more attention than other γ-secretase subunits. Numerous γ-secretase independent functions of Presenilin have been found, including calcium homeostasis, Wnt/β-catenin signaling and protein trafficking/degradation (Duggan and McCarthy, 2016). On the other hand, fewer efforts have been put in the study of other γ-secretase subunits, such as Nicastrin. Conditional knockout of *nicastrin* in mature excitatory neurons in mice results in hyperphosphorylation of Tau proteins, activation of astrocytes and microglia, progressive neuronal loss and cognitive impairments (Tabuchi et al., 2009). Furthermore, electrophysiological analysis on the hippocampal slices of the conditional *nicastrin* knockout mice revealed deficient synaptic plasticity and impaired NMDAR-mediated long term potentiation (Lee et al., 2014). These results suggest that Nicastrin plays an important role in maintaining neuronal survival and synaptic functions. However the mechanisms still need to be further clarified.

doi:10.6342/NTU201803306

1.4 Zebrafish as A Model to Study Neurodegeneration

So far, the majority of insights into neurodegeneration come from human and mouse studies. However, the complexity of mammalian nervous system has been an obstacle to untangle the mechanisms of neurodegeneration in details. Therefore, increasingly reductionistic models have been applied in neurodegeneration studies, such as *D. malenogaster* and *C. elegans*. These models have comparatively simple nervous system, which are excellent platforms to comprehensively study neurodegeneration and test experimental hypotheses. Although plenty of conclusions drawn in *D. malenogaster* or *C. elegans* system can fit into the mammalian system, these invertebrate animal models are still evolutionarily far from mammals (Schmid and Haass, 2013; Babin et al., 2014).

In the same time, *Danio rerio* which is the so-called zebrafish has been increasingly applied to study neurodegeneration for some advantages. In the beginning, zebrafish was found to be a good animal model in vertebrate development research due to its transparent embryos, which allows direct observation of developmental processes under a standard microscope. Besides, zebrafish handling is easy and economical. Next, zebrafish has high fecundity and short reproductive cycle, allowing high-throughput experiments. Various neuronal and glial cells reporter lines of zebrafish have been created to do cellular studies. Furthermore, there are various gene-modulating tools available for zebrafish. Nowadays,

doi:10.6342/NTU201803306

we can easily knockdown the expression of a specific gene by injecting morpholinos into zebrafish embryos or knock in/out certain genes from zebrafish by CRISPR-Cas9 system (Bill et al., 2009; Hruscha et al., 2013). Most importantly, zebrafish genome has been entirely sequenced and is highly homologous to human, indicating that zebrafish researches can mostly be applied to human studies. As a vertebrate animal model with simple central nervous system, using zebrafish to study neurodegeneration could fill the gap between invertebrates and mammals (Newman et al., 2014).

So far, zebrafish has been applied to model several notorious human neurodegenerative diseases, including Alzheimer's disease, Parkinson's disease, Huntington's disease, amyotrophic lateral sclerosis, etc. (Xi et al., 2011; Martín-Jiménez et al., 2015). Furthermore, using zebrafish to study neurodegeneration-related cellular pathways such as γ-secretase-mediated signaling pathways and protein degradation pathway is undergoing (Newman et al., 2014). Taken together, zebrafish is a versatile model and could help us gain more insights into neurodegeneration mechanisms.

1.5 *nicastrin*^{hi1384}

nicastrin^{hi1384} is an insertional mutation in the intron 1 of zebrafish *nicastrin* gene. This insertion derived from GT2.0 virus and depletes the expression of *nicastrin* mRNA

doi:10.6342/NTU201803306

(Amsterdam et al., 2004; Hsu, 2018). Homozygous *nicastrin*^{hi1384} zebrafish die in the larva stage and display depigmentation phenotype while many of them also have curly-up tail (Hsu, 2018). On the other hand, heterozygous *nicastrin*^{hi1384} zebrafish (*nicastrin*$^{hi1384/+}$) are phenotypically similar to wild type zebrafish and can survive for more than 2 years. As mentioned above, Nicastrin deprivation by conditional knockout in neurons leads to neurodegeneration in mice (Tabuchi et al., 2009; Lee et al., 2014). Previously, several neurodegenerative phenotypes of adult *nicastrin*$^{hi1384/+}$ zebrafish were discovered in our lab, including hyperphosphorylation of Tau proteins and cognitive impairments. It seems that *nicastrin*$^{hi1384/+}$ zebrafish could be a model to study neurodegeneration.

1.6 Specific Aim

My aim is to comprehensively examine the neurodegeneration-like phenotypes of *nicastrin*$^{hi1384/+}$ zebrafish and to evaluate if *nicastrin*$^{hi1384/+}$ zebrafish could be a neurodegeneration model.

doi:10.6342/NTU201803306

Chapter 2. Materials and Methods

2.1 Maintenance of Zebrafish

Zebrafish were maintained at 28°C with 14:10 hours light-dark cycle in the Zebrafish Core Facility of NHRI, Zhunan, Taiwan, and fed with food powder and brine shrimp twice a day respectively. Zebrafish embryos were collected after fertilization and incubated in egg water (0.03% sea salt) at 28.5°C to 5 dpf. Afterwards, larva were transferred to system water, incubated at 28°C and fed with paramecium to 30 dpf. The experimental procedures were approved by the Institutional Animal Care and Use Committee, National Health Research Institutes, Taiwan (NHRI-IACUC-100028-A, NHRI-IACUC-103122-AE and NHRI-IACUC-107094-A).

2.2 Identification of *nicastrin*$^{hi1384/+}$ Zebrafish

We used traditional alkaline lysis method to extract zebrafish's genomic DNA (Osmundson et al., 2013). In detail, zebrafish were anesthetized in 0.02% MS-222 (E10521, Sigma) and their tails were cut down, lysed in 50 mM NaOH at 95°C for 15 min. Afterwards, 1M Tris-HCl, pH8.0 was added for neutralization. Then the tail lysates were centrifuged at 2200g for 20 min at 4 °C to precipitate cell debris. Genomic DNA, PCR primers (Exon 1-1: 5'-GCGTTCAGCTTCTCATTACAGC-3'; GT2.0: 5'-

doi:10.6342/NTU201803306

CCAAACCTACAGGTGGGGTC-3'; Intron1-1: 5'-CTACCCGAAGAGACGTTCAG T-3') (Figure 1) and 2X PCR One mix (SM203-0100, GeneDireX) were mixed and total volume for each sample was adjusted to 20 μl with ddH_2O. PCR was carried out in a thermal cycler. The program was that 94°C for 3 minutes to preheat and break down hydrogen bonds of DNA, followed by 34 cycles of 94°C for 30 seconds, 60°C for 30 seconds and 72°C for 30 seconds to amplify PCR products and then 72°C for 4 minutes for final extension, in the end, the temperature was maintained at 10°C. PCR products were separated in 1% or 2% agarose gel with 10% ethidium bromide (EtBr) by gel electrophoresis. DNA fragments within gel were detected by UV light in a gel imager system.

2.3 Visual Motor Response Tests

For zebrafish larva visual motor response (VMR) tests, embryos were collected 1 hours after fertilization. Afterwards, 60 subject zebrafish embryos were transferred to a petri dish containing egg water and incubated at 28°C with 14:10 light-dark cycle. Egg water was changed every day. While the subject zebrafish grew to 5 dpf, they were transferred to a 99 well plate with 650 μl egg water. VMR tests were conducted in DanioVision^{TM} Observer Chamber (Noldus) with 3 hours for dark adaptation and followed by 3 times of 30:30 minutes light-dark cycle (Figure 3). Movements of subject

doi:10.6342/NTU201803306

zebrafish larva were recorded and live analyzed by Ethovision XT13 (Noldus). Afterwards, *nicastrin*$^{hi1384/+}$ zebrafish larva or wild type siblings were identified by using the extracted genomic DNA from whole larva for genotyping.

2.4 Sampling of Adult Wild Type and *nicastrin*$^{hi1384/+}$ Zebrafish for T-maze Behavioral Tests

As we fed comparatively more food to experimental zebrafish to accelerate growth, more zebrafish became female in the process. Furthermore, previous mice study suggested neurodegeneration phenotypes were more significant in female than in male (Katia et al., 2013). Accordingly, We focused on female zebrafish in T-maze behavioral tests, microarray, qPCR, H&E staining and TUNEL staining experiments.

2.5 Zebrafish T-maze Behavioral Tests

For T-maze behavioral tests, subject fish were genotyped at least 3 weeks before they entered behavioral experiment trials. The behavioral experiment trials contained 5 days of pre-training, 2 days of starvation, 5 days of training and 1 day of test in the end (Figure 2A). During pre-training phase, 10-15 subject fish with same genotype were put in a 3L tank and fed with food-containing sponge cubes twice a day. In the end of pre-training phase, the subject zebrafish were isolated and genotype-blinded. After 2 days of starvation,

doi:10.6342/NTU201803306

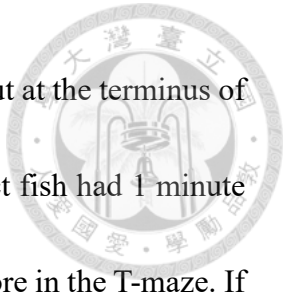

individual fish was trained to find the food-containing sponge cube put at the terminus of left arm in a T-maze (Figure 2C). In the beginning of training, subject fish had 1 minute for acclimation in start zone. Afterwards, it would be allowed to explore in the T-maze. If the fish successfully found the food cube and ate the food, the latency (time) would be recorded and the fish would get 30 seconds to stay in the T-maze and enjoy the food. Alternatively, if the subject fish failed to find the food cube in 2 minutes, it would be recorded as "fail" and the fish would be chased to the food cube location and stay for 30 seconds. In the final test, a sponge cube without food was put in the same location as training session, and behaviors of individual zebrafish was tested with 1 minute for acclimation and two minutes for exploration (Figure 2D). The movement of zebrafish in the T-maze during test phase was recorded with a monitoring camera (KMS-63F119HN). The recorded videos were analyzed by Ethovision XT13 (Noldus). Latency to find the food cube in the T-maze was the parameter to measure learning and memory ability. Learning behavior was analyzed by data from training sessions, while test data was used to analyze memory of subject zebrafish.

2.6 Statistics of Zebrafish T-maze Behavioral Tests Data

First of all, Grubb's test was applied to remove outliers for each group of data. The function of Grubbs'test as follows

doi:10.6342/NTU201803306

$$G_{cal} = \frac{Questionable\ \ data - \bar{X}}{s}$$

where $\bar{X}$ is average, and s is standard deviation.

If and only if when G_{cal}>G_{table}, $Questionable\ \ data$ could be considered as an outlier. The value of G_{table} was referred to Table 2.

Next, Cox proportional hazard model was used to assay the difference between two groups. Because the velocity varied from fish to fish, our T-maze behavioral tests results might be confounding with this variable. It is desirable to adjust for the velocity in Cox model. In addition, as there was a censoring time when we recorded the latency for subject zebrafish to arrive at the food location, survival analysis was conducted to determine the significance of difference. More specifically, let T_i (Test Latency) denote the survival time of the ith fish and censoring time is 120 sec. Let V_i, and G_i be the velocity, and group index of ith fish, respectively. Note that $G_i = 1$ if and only if heterozygous in the ith fish. We consider a Cox proportional hazard function as follows

$$\lambda_0(t)exp\{\beta_V V_i + \beta_G G_i\},$$

where $\lambda_0(t)$ is a baseline hazard function.

2.7 Microarray

2.4-1 Sampling

doi:10.6342/NTU201803306

To exclude the influence of variation in cognitive ability in the same genotype, we ranked the performance of subject wild type and *nicastrin*$^{hi1384/+}$ zebrafish of T-maze behavioral tests respectively according to latency in test phase. Afterwards, we chose 5 subject zebrafish whose ranking were separated at an interval for each genotype as samples of microarray experiments.

2.4-2. Brain Dissection

Sample fish which had gone through the behavioral trials were anesthetized as mentioned and their brains were dissected out on a cold ice pack, and then preserved in RNA*later*™ stabilization solution (AM7020, Invitrogen™) until RNA extraction.

2.4-3. RNA Extraction

After removal of RNA*later*™ stabilization solution, 5 brains were homogenated in RNAzol (Molecular Research Center, Inc.) together for each genotype. After homogenation, Nuclase-free water (Invitrogen™) was added and centrifugation was applied to precipitate genomic DNA and proteins. After transferring the supernatant to a new Eppendorf vial respectively, isopropanol was added to precipitate total RNA and then stored at -20°C overnight. After centrifugation, RNA pellets were washed with 75% ethanol twice and then eluted with RNase-free water.

2.4-4. DNase I Treatment and Cleanup

doi:10.6342/NTU201803306

Extracted RNA were treated with Turbo™ DNase (AM2238, Invitrogen™) for 30 minutes at 37°C to remove remaining genomic DNA and followed by clean-up with RNeasy Mini kit (74104, Qiagen). After RNA clean-up, RNA were ready for microarray experiments.

2.4-4 Microarray

After RNA quality control by Bioanalyzer 2100 (Agilent Technologies, Santa Clara, CA, USA), gene expression microarray experiments were performed with Affymetrix Zebrafish Gene 1.0 ST Array by Microarray Core Laboratory of NHRI. The microarray data were normalized by a robust multiarray averaging (RMA) algorithm. Gene lists were created by conducting ANOVA on normalized data with Partek Genomics Suite (Partek Inc., Saint Louis, MO, USA). Disease and functional analysis of significantly affected genes ($p<0.05$; FDR<0.05) was done by IPA (Ingenuity Systems Inc., Redwood City, CA).

2.8 Quantitative Real-time PCR

Brain dissection and RNA extraction methods are described above. After total RNA extraction, reverse-transcription was performed to synthesize cDNA by following the instruction of SuperScriptTM III First-Strand Synthesis System (18080051, InvitrogenTM). The synthesized cDNA were stored in -20°C until use. The quantitative real-time PCRs were conducted with Fast SYBR® Green Master Mix (Applied

doi:10.6342/NTU201803306

Biosystem) in LightCycler® 480 Instrument II (Roche). The sequence of primers are listed in Table 1. qPCR program was 95°C for 5 minutes, followed by 45 cycles of 95°C for 10 seconds, 68°C for 10 seconds, and 72°C for 10 seconds. *rps24* was used for an internal control.

2.9 H&E Staining

For H&E staining, subject zebrafish were anesthetized in overdosed MS-222 and their heads were cut off, washed in 1X PBS and then fixed in 4% PFA at 4°C for a week. After washing with 1X PBS, the heads were decalcified in 15% EDTA. After dehydration in 30%, 50% and 70% ethanol, decalcified zebrafish heads were delivered to the Pathology Core Laboratory of NHRI for paraffin embedding. 5 μm sections were cut using a Leica RM2135 rotary microtome and delivered to the Pathology Core Laboratory of NHRI for standard H&E staining. Pictures were taken by Zeiss Axio Imager A1.

2.10 TUNEL Staining

For TUNEL staining, subject zebrafish were anesthetized in 0.02% MS-222 and their heads were cut off, washed in 1X PBS and then fixed in 4% PFA at 4°C overnight. Afterwards, the brains were dissected out from the head, washed in 1X PBS, immersed in 15% sucrose for 3 hours and then 30% sucrose overnight at 4°C。Then the brains were embedded in O.C.T (Tissue-Tek O.C.T Compound, Sakura, 4583) and 15 μm

doi:10.6342/NTU201803306

cryosections were cut using a Thermo Shandon Cryotome E Cryostat. TUNEL staining was performed following the instructions from In Situ Cell Death Detection Kit, Fluorescein (Roche). Pictures were taken under a confocal microscope with Leica TCS Sp5 system.

doi:10.6342/NTU201803306

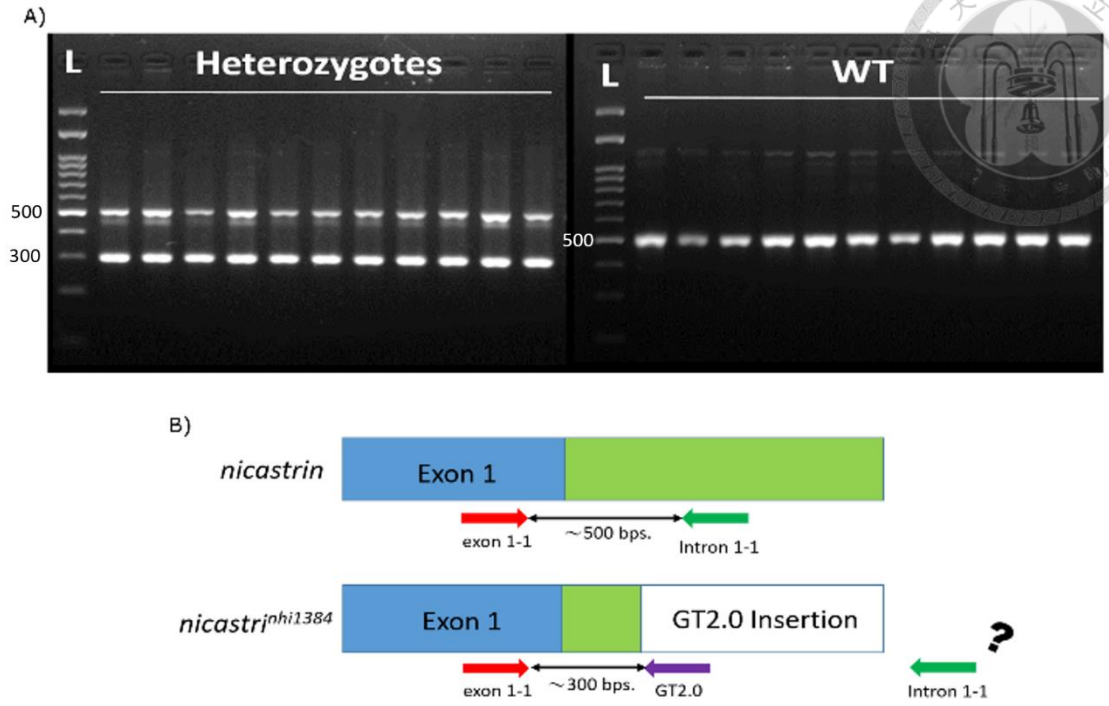

Figure 1. Genotyping of *nicastrin*$^{hi1384/+}$

(A) Gel electrophoresis of PCR products from wild type and *nicastrin*$^{hi1384/+}$ zebrafish tissues. PCR products of wild type zebrafish only contain 500 bps DNA fragments, while that of *nicastrin*$^{hi138/+4}$ zebrafish contain both 300 and 500 bps DNA fragments. (B) *exon1-1*, *intron 1-1* and *GT2.0* are primers designed for *nicastrin*^{hi1384} allele genotyping.

doi:10.6342/NTU201803306

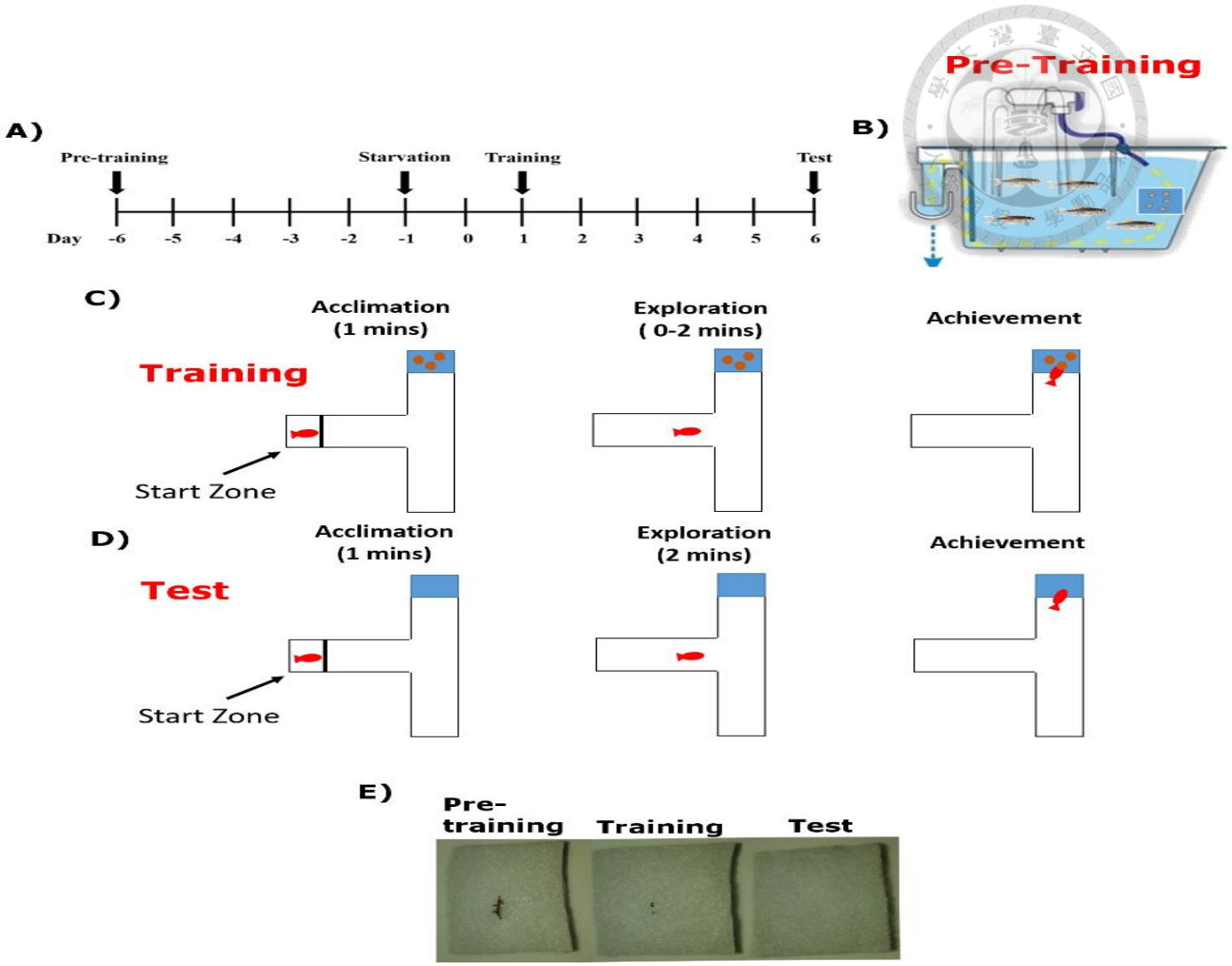

Figure 2. Scheme of T-maze Behavioral Test

(A) The schedule of T-maze behavioral test contains 5 days of pretraining, 2 days of starvation, 5 days of training and 1 day of test. (B-D) Schematic pictures for pretraining (B), training (C) and test (D) phase of T-maze behavioral test are shown (E) Sponge cubes were used in pretraining, training, and test phase of T-maze behavioral test are shown.

doi:10.6342/NTU201803306

Table 1. List of Primers for Quantitative Real-time PCR

Target	Primer Type	Sequence
rps24	Forward	5'-TGGTGTTCGTCTTTGGCTTCA-3'
	Reverse	5'-ATGCCTCTAACTTTCTTCATTCTGTTC-3'
nicastrin	Forward	5'-ATGGAGAAGCAGGTGTCAGAGAT-3'
(Lim et al., 2015)	Reverse	5'-TCTCAGAAATCGCTGGAAGGA-3'
presenilin 1	Forward	5'-TTCCCAGCGCTCATCTACTC-3'
	Reverse	5'-GGGAGCCATCGCAACTACCT-3'
oxytocin	Forward	5'-CCATTCGACAGTGTATGCCGTG-3'
	Reverse	5'-CATCTCACACGGAGAAGGGAGA-3'
clca1	Forward	5'-GCTGAAACCGCAGAGCCTGGA-3'
	Reverse	5'-GCTGGTTCATGCGGGTTTTGACA-3'

Table 2. G_{table} Values of Grubb's Test

Number of Observations	Confidence Level (%)			
n	99.5	99	95	90
3	1.155	1.155	1.153	1.148
4	1.496	1.492	1.463	1.425
5	1.764	1.749	1.672	1.602
6	1.973	1.944	1.822	1.729
7	2.139	2.097	1.938	1.828
8	2.274	2.221	2.032	1.909
9	2.387	2.323	2.11	1.977
10	2.482	2.41	2.176	2.036
11	2.564	2.485	2.234	2.088
12	2.636	2.55	2.285	2.134
13	2.699	2.607	2.331	2.175
14	2.755	2.659	2.371	2.213
15	2.806	2.705	2.409	2.247

Source: ASTM E178-00. "Standard Practice for Dealing with Outlying Observations"

doi:10.6342/NTU201803306

Chapter 3. Results

3.1 Behavioral Tests On *nicastrin*$^{hi1384/+}$ Zebrafish Larva

The importance of *nicastrin* gene in neuronal survival and functions has been revealed (Tabuchi et al., 2009; Lee et al., 2014). Although *nicastrin*$^{hi1384/+}$ zebrafish are phenotypically similar to their wild type siblings, their behaviors might be different. Thus, I conducted the visual motor response test on wild type and *nicastrin*$^{hi1384/+}$ zebrafish larva at 5 days post fertilization. The visual motor response (VMR) test was designed to examine the mobility of zebrafish larva and their response to sudden light or dark stimulus (Emran et al., 2008). The velocity of wild type and *nicastrin*$^{hi1384/+}$ zebrafish larva were not significantly different which were measured by movement of the center point of the animal. However, the activity of *nicastrin*$^{hi1384/+}$ zebrafish larva was increased in the light-on period (Figure 3), which was measured by pixel changes in the entire arena, indicating that *nicastrin*$^{hi1384/+}$ zebrafish larva are more activated under light stimulus. On the other hand, ablation of *nicastrin* gene expression in homozygous *nicastrin*^{hi1384} zebrafish leads to degeneration of retinal pigment epithelium (RPE), which might compromise vision (Hsu et al., 2018, Ph.D Thesis). Nevertheless, *nicastrin*$^{hi1384/+}$ zebrafish larva could react to light and dark stimulus as quickly as their wild type siblings, implicating that

doi:10.6342/NTU201803306

nicastrin$^{hi1384/+}$ zebrafish larva have normal vision. In conclusion, *nicastrin*$^{hi1384/+}$ zebrafish larva can react normally to sudden light or dark stimulus and have higher activity than wild type siblings under light exposure.

3.2 Adult *nicastrin*$^{hi1384/+}$ zebrafish have intact retina

As mentioned above the retinal pigment epithelium is impaired in homozygous *nicastrin*^{hi1384} zebrafish but not in wild type or *nicastrin*$^{hi1384/+}$ zebrafish larva (Hsu, 2018). Given the role of gamma-secretase functions in melanosome formation, the RPE layer of *nicastrin*$^{hi1384/+}$ zebrafish might degenerate as they grow up. As a result, I carried out hematoxylin and eosin staining on the eye sections of wild type and *nicastrin*$^{hi1384/+}$ zebrafish at 3 month, 6 month, and 14 month of age (Figure 4). No deficit in the RPE layers of *nicastrin*$^{hi1384/+}$ zebrafish at these three ages was found, suggesting that adult *nicastrin*$^{hi1384/+}$ zebrafish have intact retina structure.

3.3 T-maze Behavioral Tests on *nicastrin*$^{hi1384/+}$ zebrafish

Preliminary data had suggested aged *nicastrin*$^{hi1384/+}$ zebrafish have learning and memory deficits in a T-maze behavior test (unpublished data). We intended to find out when the *nicastrin*$^{hi1384/+}$ zebrafish start to show cognitive decline. Therefore, adult wild type or *nicastrin*$^{hi1384/+}$ zebrafish at 3, 6, 12 and 18 months of age were applied to T-maze

doi:10.6342/NTU201803306

behavior tests as described above (Figure 2). Given that there was a censoring time in the T-maze behavioral tests (120 seconds), we used cox proportional hazard model to do statistical analysis. In addition, there are some other factors might also contribute to the results, such as mobility. Therefore, we made an adjustment for the velocity to exclude the influence caused by variation in mobility of subject fish in our statistical model (Chapter 2.6). The latency of finding food decreased through the training sessions (Figure 5), indicating that the subject fish could learn where to find the food in the training phase of T-maze behavioral test. In addition, no significant difference in the finding-food latency between wild type and *nicastrin*$^{hi1384/+}$ zebrafish at these four ages, which suggested no significant difference in the learning behavior between wild type and *nicastrin*$^{hi1384/+}$ zebrafish in 18 month of age (Figure 5). On the other hand, in the test phase, the latency of wild type and *nicastrin*$^{hi1384/+}$ zebrafish at 3 and 6 month of age were not significant, while the difference in finding-cube latency got more significant between wild type and *nicastrin*$^{hi1384/+}$ zebrafish at 12 and 18 month of age (Figure 6). This data implicated that *nicastrin*$^{hi1384/+}$ zebrafish suffer from age-dependent memory deficits.

Another factor that could affect the performance of subject fish in the T-maze behavioral test is vision. There is no solid evidence suggesting that the vision of *nicastrin*$^{hi1384/+}$ zebrafish is normal despite that H&E staining displayed that no deficit appeared in the eyes of *nicastrin*$^{hi1384/+}$ zebrafish (Figure 4). Moreover, *nicastrin*$^{hi1384/+}$

doi:10.6342/NTU201803306

zebrafish larva could react to sudden light or dark stimulus as wild type fish (Figure 3). Taken together, we think the significant difference in performance of wild type and *nicastrin*$^{hi1384/+}$ zebrafish in the T-maze behavioral test was mostly attributed to cognitive ability but not vision.

Original T-maze behavioral test showed that *nicastrin*$^{hi1384/+}$ zebrafish have age-dependent memory deficits. However, we could not recapitulate this result. The latter T-maze behavioral tests on 6 month wild type and *nicastrin*$^{hi1384/+}$ zebrafish still showed no significant difference in learning and memory, whereas latter T-maze behavioral test data on 12 and 18 month wild type and *nicastrin*$^{hi1384/+}$ zebrafish were not significant, which was inconsistent to the original T-maze behavioral tests (Supplementary Figure 1). One possible reason is that we used different food in the latter T-maze behavioral test, because the former food had been run out and unavailable. Therefore, the distinct behavioral experiments results require further examination by a new behavioral test platform.

Conclusively, original T-maze behavioral data suggested that *nicastrin*$^{hi1384/+}$ zebrafish have age-dependent memory decline, which could not be owed to discrepancy in mobility or retinal structure. However, the fact that we failed to repeat the previous result makes it ambiguous to draw the conclusion. More efforts have to be made to address this problem, which will be discussed later.

doi:10.6342/NTU201803306

3.4 Transcriptomic Analysis On Adult *nicastrin*$^{hi1384/+}$ Zebrafish

To find out the mechanisms or which pathways are affected in the brains of adult *nicastrin*$^{hi1384/+}$ zebrafish that can lead to age-dependent memory deficits, we used microarray to analyze the transcriptome of the brains of subject wild type and *nicastrin*$^{hi1384/+}$ zebrafish which had gone through original T-maze behavioral test. There were 37669 genes analyzed in the microarray chip, and we found expression levels of 6733 (upregulation and downregulation), 5486 (upregulation and downregulation), 2206 (upregulation and downregulation) genes were significantly affected ($p<0.05$ and FDR <0.05) in *nicastrin*$^{hi1384/+}$ zebrafish at 3, 6 and 18 month of age respectively (Figure 7A-B). By conducting disease and functional analysis on these affected genes, we found neurodegeneration associated phenotypes were predicted to be activated in aged *nicastrin*$^{hi1384/+}$ zebrafish while neuronal survival and functions associated phenotypes were predicted to be inhibited (Figure 7C). The result suggested that *nicastrin*$^{hi1384/+}$ zebrafish suffer from age-dependent neurodegeneration at transcriptional level.

In the following, we desired to know whether the subject *nicastrin*$^{hi1384/+}$ zebrafish of latter behavioral tests showed age-dependent neurodegeneration as well in spite of the failure to recapitulate original T-maze behavioral test results of age-dependent memory deficits. We also conducted transcriptomic analysis by microarray on the subject zebrafish of latter behavioral experiments. The results showed that expression levels of 1628 (774

doi:10.6342/NTU201803306

genes upregulated and 854 genes downregulated), 5654 (3629 genes upregulated and 2025 genes downregulated) and 2246 genes (971 genes upregulated and 1275 genes downregulated) were affected ($p<0.05$ and FDR<0.05) in the brains of *nicastrin*$^{hi1384/+}$ zebrafish compared to wild type zebrafish at 6, 12, and 18 month of age respectively (Supplementary Figure 2A-B). Furthermore, disease and functional analysis also displayed similar age-dependent neurodegeneration patterns in subject *nicastrin*$^{hi1384/+}$ zebrafish of latter behavioral experiments. In summary, transcriptomic analysis showed *nicastrin*$^{hi1384/+}$ zebrafish has age-dependent neurodegeneration at transcriptional level.

3.5 Validation of Microarray Results by Quantitative Real-time PCR

Homozygous *nicastrin*^{hi1384} mutation abrogates the expression of *nicastrin* mRNA in zebrafish larva. However, the expression level of *nicastrin* mRNA in the brains of *nicastrin*$^{hi1384/+}$ zebrafish had not been explored yet. I specifically looked into the expression level of *nicastrin* mRNA in microarray results and found that *nicastrin* mRNA expression in the brains of *nicastrin*$^{hi1384/+}$ zebrafish was downregulated (Figure 8A). In addition, there are several reports suggesting that the expressions of γ-secretase subunits are interconnected (Steiner et al., 2002). However, the mRNA expression of other γ-secretase subunits in *nicastrin*$^{hi1384/+}$ zebrafish, including presenilin 1, presenilin 2, aph-1 and pen-2, were not significantly different from wild type despite the downregulation of

doi:10.6342/NTU201803306

nicastrin mRNA (Figure 8B-E). Next, we used qPCR to verify the microarray results and found that *nicastrin* mRNA expressions decreased in *nicastrin*$^{hi1384/+}$ zebrafish, especially at 12 and 18 month of age, which is consistent to age-dependent neurodegeneration showed in transcriptomic analysis (Figure 9A). Interestingly, *nicastrin* expressions of both wild type and *nicastrin*$^{hi1384/+}$ zebrafish at 6 month were siginifcantly lower compared to other age, implicating that expression of *nicastrin* in the zebrafish brain is age-dependent (Figure 9A). On the other hand, there was no significant difference in the *presenilin-1* mRNA expression between wild type and *nicastrin*$^{hi1384/+}$ zebrafish at the same age (Figure 9B). Besides, the expressions of *presenilin-1* were significantly downregulated in 18 month wild type and *nicastrin*$^{hi1384/+}$ zebrafish (Figure 9B).

Additionally, disease and functional analysis of both original and latter microarray data showed 18 month *nicastrin*$^{hi1384/+}$ zebrafish have neurodegeneration at transcriptional level. Therefore, I picked two genes, *oxt* and *clca1* from the microarray results and conducted qPCR for verification. These two genes have been implicated to involve in neurodegeneration and their expressions are significantly affected in the brains of 18 month *nicastrin*$^{hi1384/+}$ zebrafish in both original and latter microarray results. *oxt* gene encodes oxytocin, which is known as a hormone secreted from hypothalamus carries neuroprotection effects (Tanyeri et al., 2015; Kaneko et al., 2016), and was downregulated in 18 month *nicastrin*$^{hi1384/+}$ zebrafish brain shown by microarray and qPCR (Figure 10A,

doi:10.6342/NTU201803306

B). On the other hand, *clca1* gene encodes Calcium-activated Chloride Channel Regulator, has been reported to participate in glutamate-induced excitotoxicity (Zhang et al., 2007; Wahl et al., 2009), and was upregulated in 18 month *nicastrin*$^{hi1384/+}$ zebrafish brain in our microarray and qPCR results (Figure 10A, C).

Conclusively, both microarray and qPCR display that *nicastrin* mRNA expression was reduced in the brains of *nicastrin*$^{hi1384/+}$ zebrafish. Furthermore, *oxt* mRNA was downregulated and *clca1* mRNA was upregulated in 18 month *nicastrin*$^{hi1384/+}$ zebrafish brain, which might together lead to neuronal loss.

3.6 Detection of Apoptosis in Telecephalons of *nicastrin*$^{hi1384/+}$ Zebrafish

As transcriptomic analysis demonstrated that *nicastrin*$^{hi1384/+}$ zebrafish have age-dependent neurodegeneration at transcription level, we wondered if there are severe neuronal apoptosis in *nicastrin*$^{hi1384/+}$ zebrafish brains. The telecephalon of zebrafish is homologue of the cerebrum of mammals, which is essential for cognitive ability. Accordingly, I conducted TUNEL staining on the telecephalon sections of wild type and *nicastrin*$^{hi1384/+}$ zebrafish at 18 month of age. There were very few TUNEL signals on both 18 month wild type and *nicastrin*$^{hi1384/+}$ zebrafish (Figure. 11), indicating that no severe neuronal apoptosis appears in the telecephaon of *nicastrin*$^{hi1384/+}$ zebrafish at 18 month of age.

doi:10.6342/NTU201803306

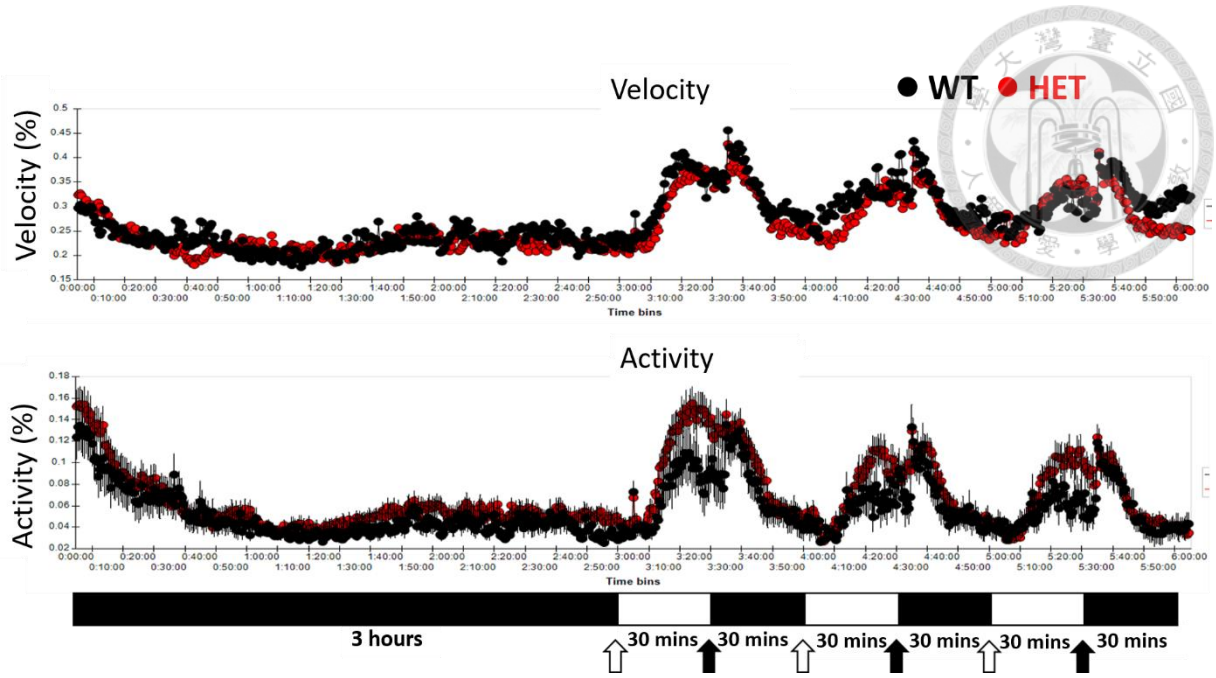

Figure 3. Visual Motor Response Test on 5 dpf Zebrafish Larva

Visual motor response test consisted of 3 hours of dark adaptation, and 3 times of 30-minutes-light and 30-minutes-dark cycles. There is no significant difference in velocity between wild type and *nicastrin*$^{hi1384/+}$ zebrafish larva. On the other hand, the activity of *nicastrin*$^{hi1384/+}$ zebrafish larva during light period was higher than wild type zebrafish larva. (WT: n=12 ; Het: n=27)

doi:10.6342/NTU201803306

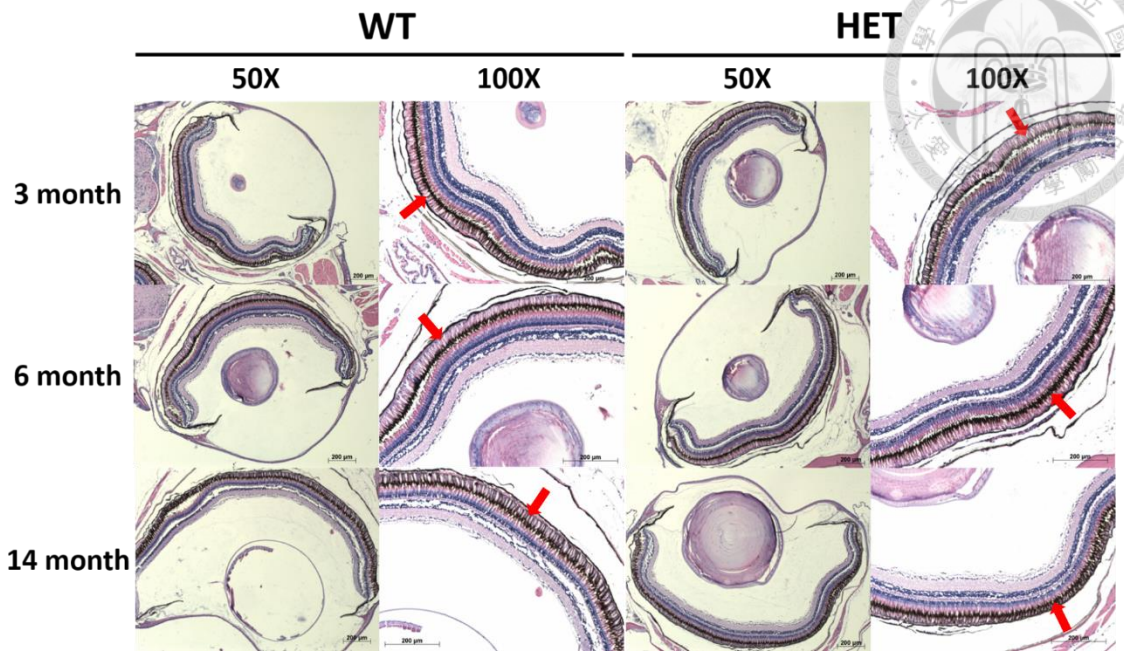

Figure 4. Retinal Structure of Adult Wild type and *nicastrin*$^{hi1384/+}$ Zebrafish

H&E staining displayed that the retinal structure of *nicastrin*$^{hi1384/+}$ zebrafish is similar to that of wild type zebrafish at 3, 6 and 14 month of age and no deficit was found in the RPE layer (red arrows) of both wild type and *nicastrin*$^{hi1384/+}$ zebrafish at these three ages. (WT: n=3; Het: n=3)

doi:10.6342/NTU201803306

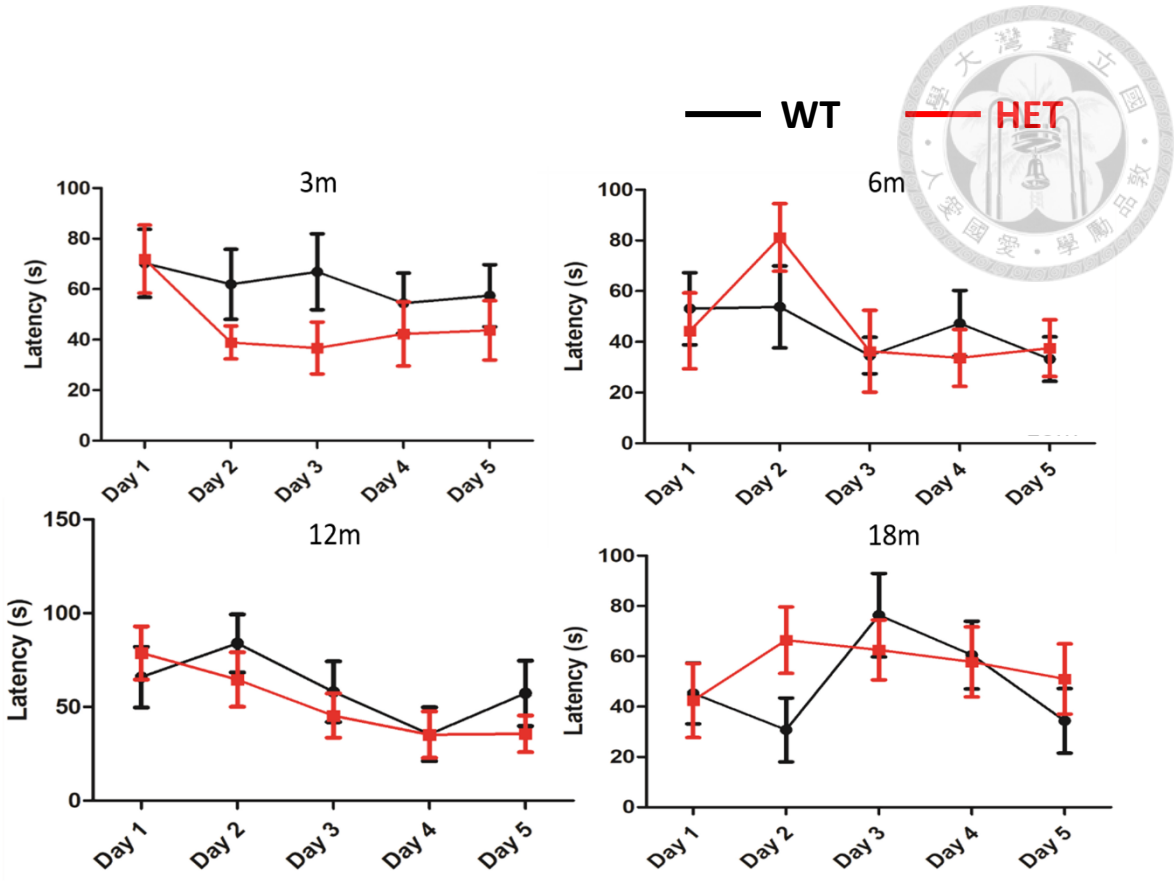

Figure 5. Learning Curves in Training Phase of Original T-maze Behavioral Tests

Learning curves of both wild type and *nicastrin*$^{hi1384/+}$ zebrafish at 3, 6, 12, and 18 month of age showed they learned where to find the food cube in the T-maze, as the latency decreased through the training sessions. However, the learning curves of 6 and 18 month subject fish were atypical because the latency on the first day of training phase was decreased, which will be discussed in Chapter 4. No significant difference in learning curve was found between wild type and *nicastrin*$^{hi1384/+}$ zebrafish at these four ages. (3m: WT: n=11; HET: n=11. 6m: WT: n=11; HET: n=8. 12m: WT: n=10; HET: n=12. 18m: WT: n=7; HET: n=9)

doi:10.6342/NTU201803306

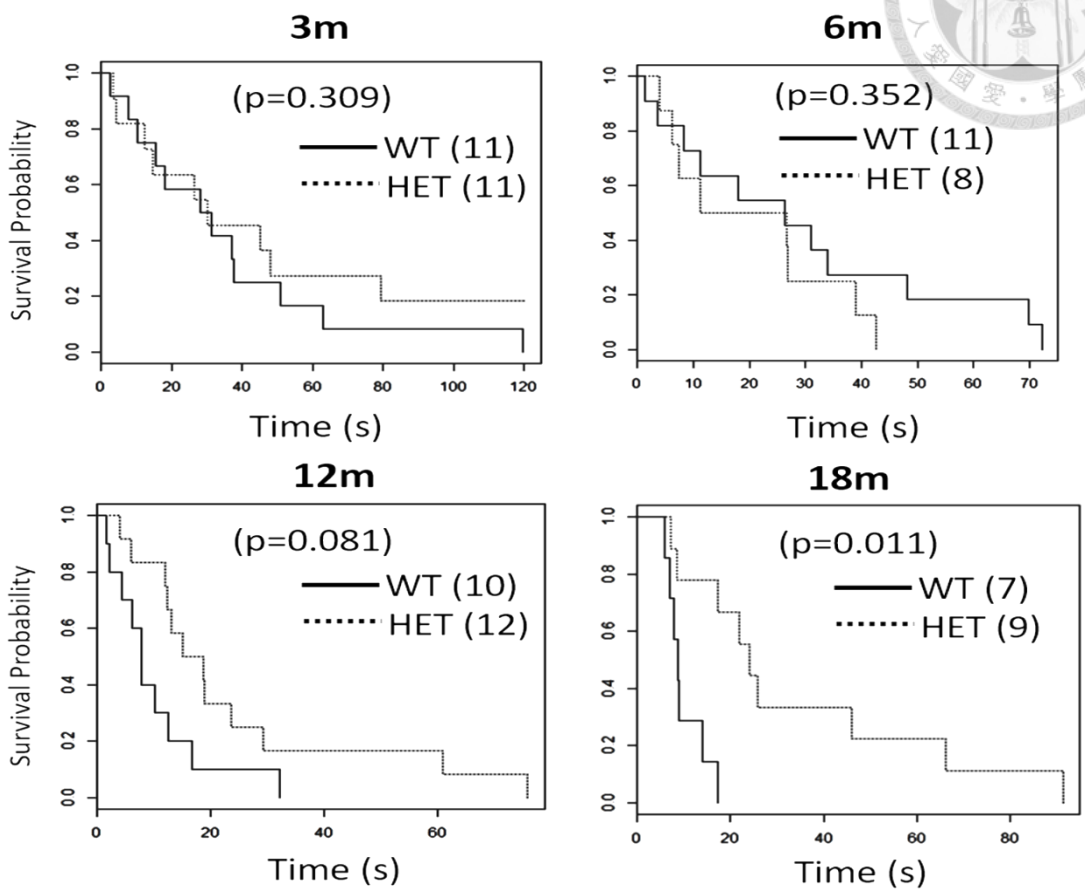

Figure 6. Latency in Test Phase of Original T-maze Behavioral Tests

The latency in test phase was not significant different between wild type and *nicastrin*$^{hi1384/+}$ zebrafish at 3 and 6 month of age. At 12 month of age, the latency of wild type zebrafish was significantly shorter than *nicastrin*$^{hi1384/+}$ zebrafish and the difference became more significant at 18 month of age.

doi:10.6342/NTU201803306

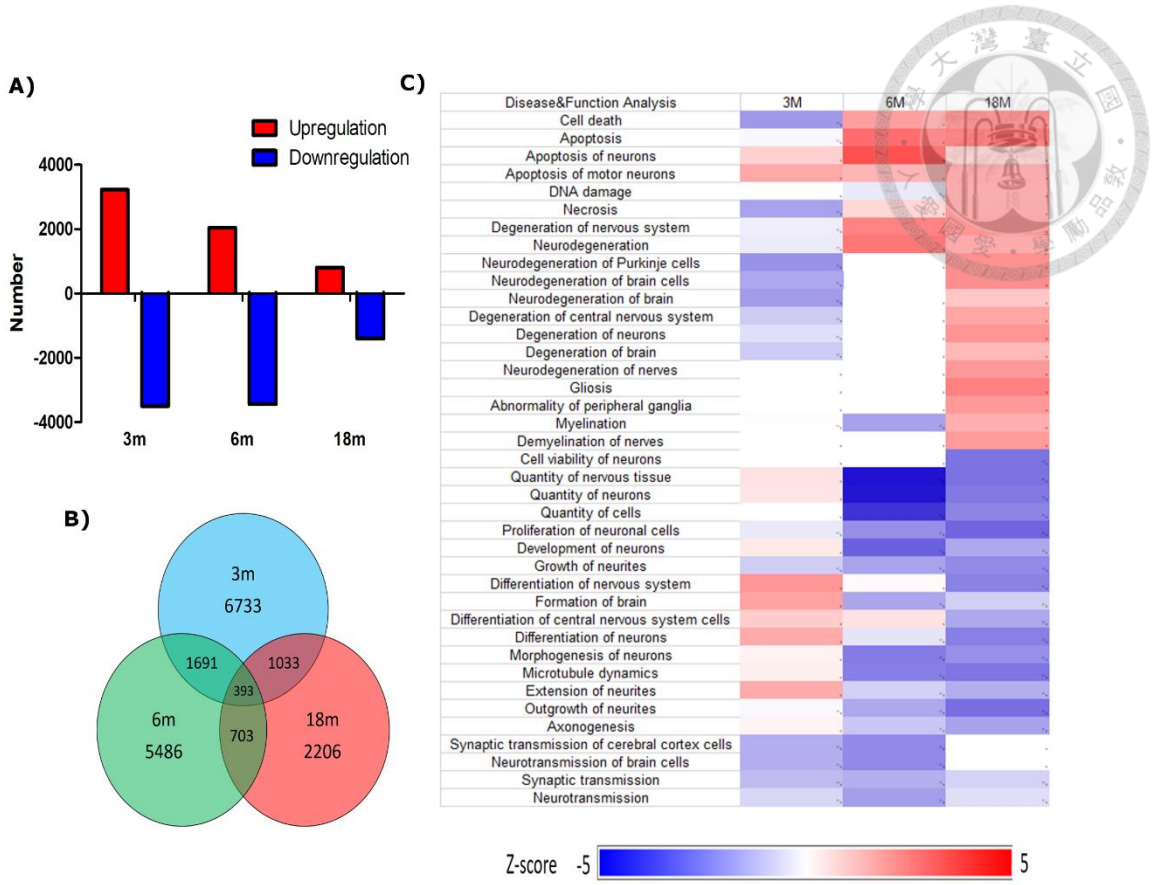

Figure 7. Transcriptomic Analysis on Subject Zebrafish of Original T-maze Behavioral Tests

(A) Overview of Microarray Data. (B) Venn Diagram of Total Number of Affected Genes In The Microarray Data (C) Neurodegeneration were predicted to be activated and neuronal survival and functions were predicted to be inhibited in aged *nicastrin*$^{hi1384/+}$ zebrafish.

doi:10.6342/NTU201803306

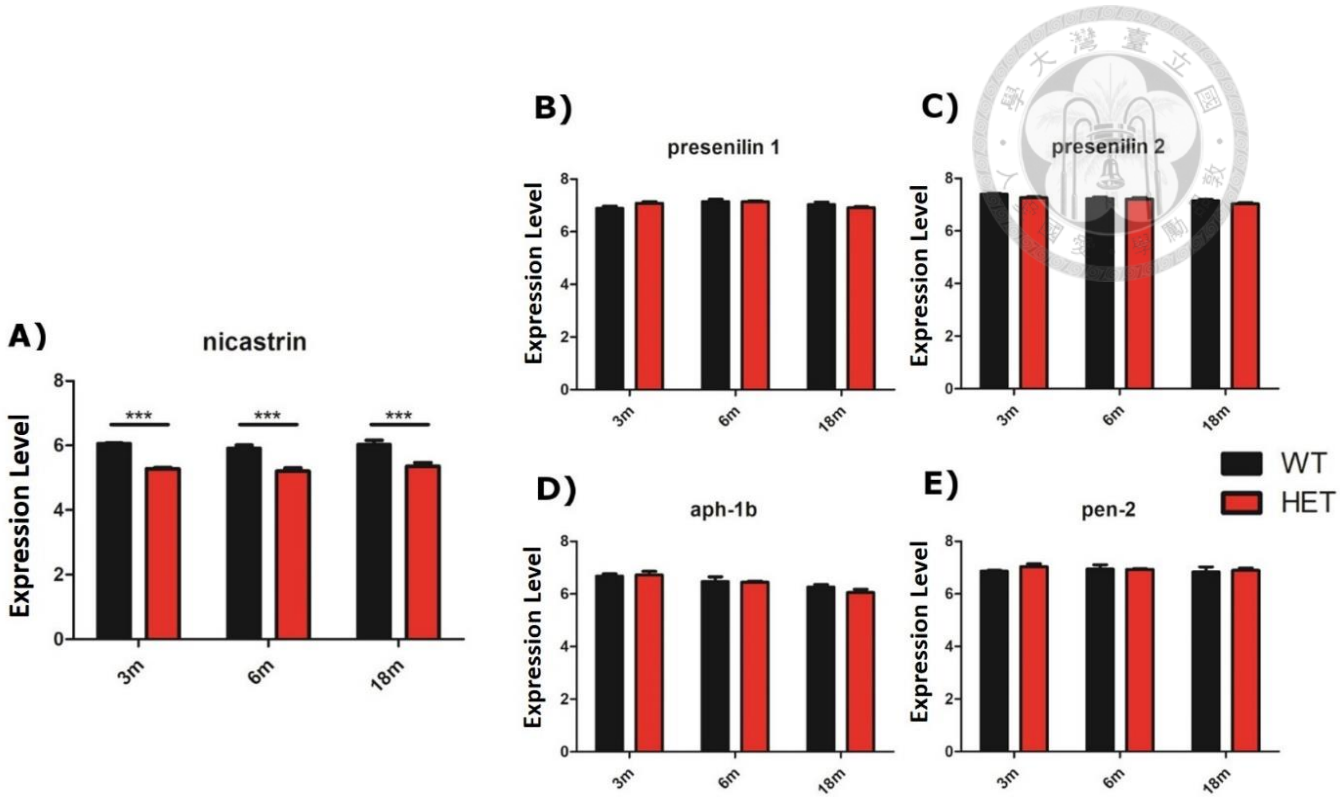

Figure 8. mRNA Levels of γ-secretase Subunits in Microarray Data

mRNA levels of *nicastrin* (A) were decreased in *nicastrin*$^{hi1384/+}$ zebrafish while mRNA levels of other γ-secretase subunits (*presenilin-1* (B), *presenilin-2* (C), *aph-1* (D), *pen-2* (E)) were not affected in microarray data.

doi:10.6342/NTU201803306

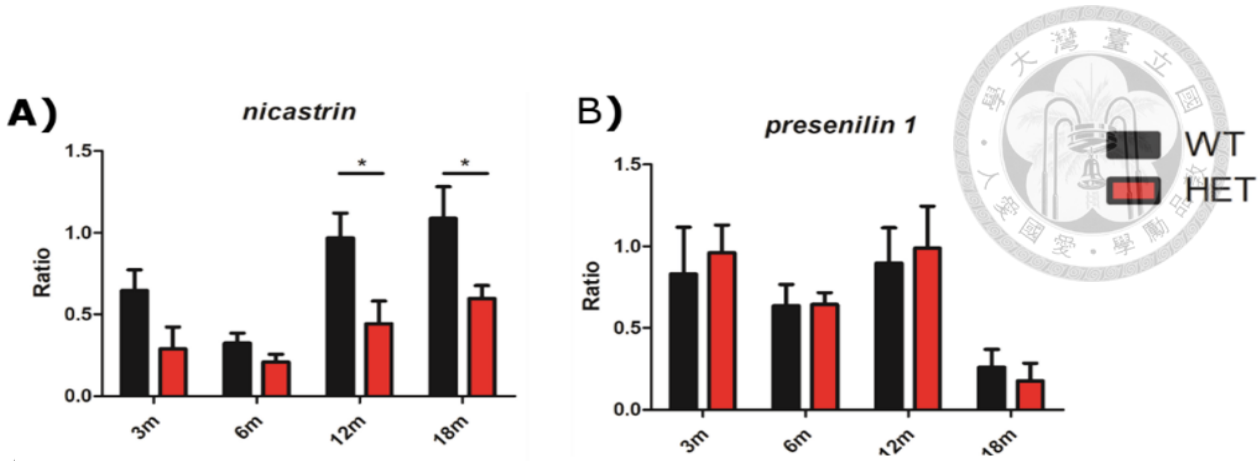

Figure 9. mRNA Levels of *nicastrin* And *presenilin-1* in qPCR Experiments

(A) Expression level of *nicastrin* was decreased in *nicastrin*$^{hi1384/+}$ zebrafish's brains, especially at 12 and month of age. (B) No difference in expression level of *presenilin-1* appeared between wild type and *nicastrin*$^{hi1384/+}$ zebrafish's brains at the same age.

doi:10.6342/NTU201803306

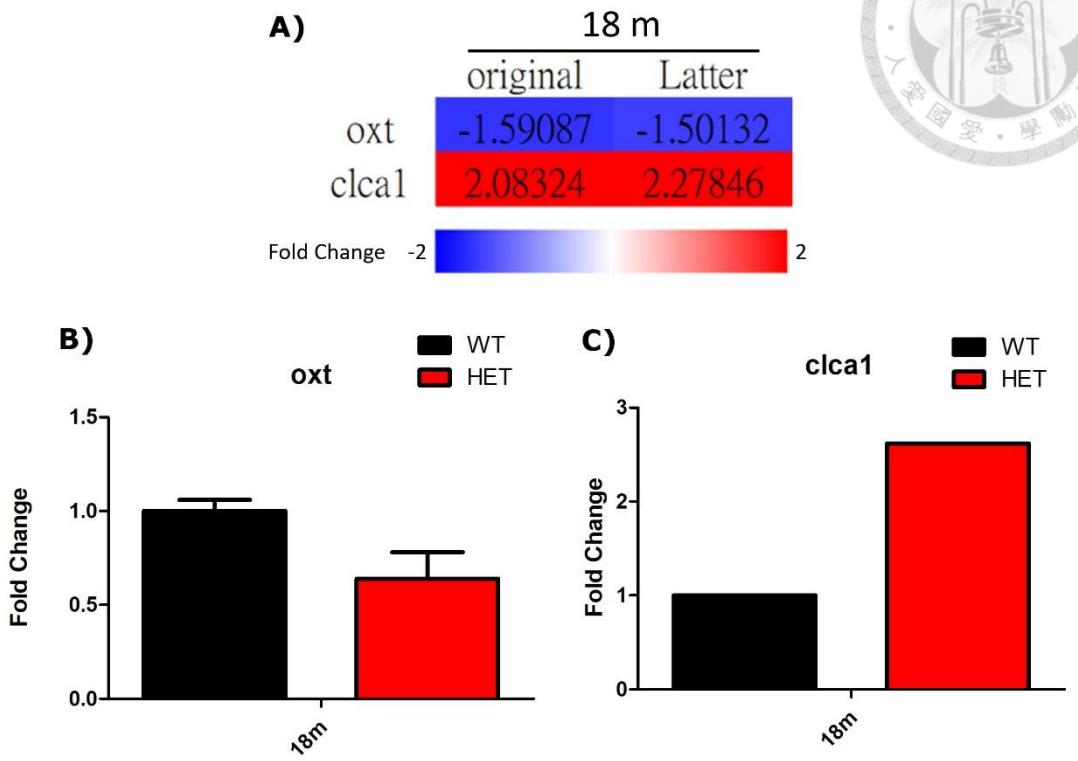

Figure 10. mRNA Levels of *oxt* And *clca1* in Microarray and qPCR Experiments

(A) Fold Change of *oxt* and *clca1* mRNA Levels in Microarray Data (B-C) Fold Change of *oxt* and *clca1* mRNA Levels in qPCR Experiments.

doi:10.6342/NTU201803306

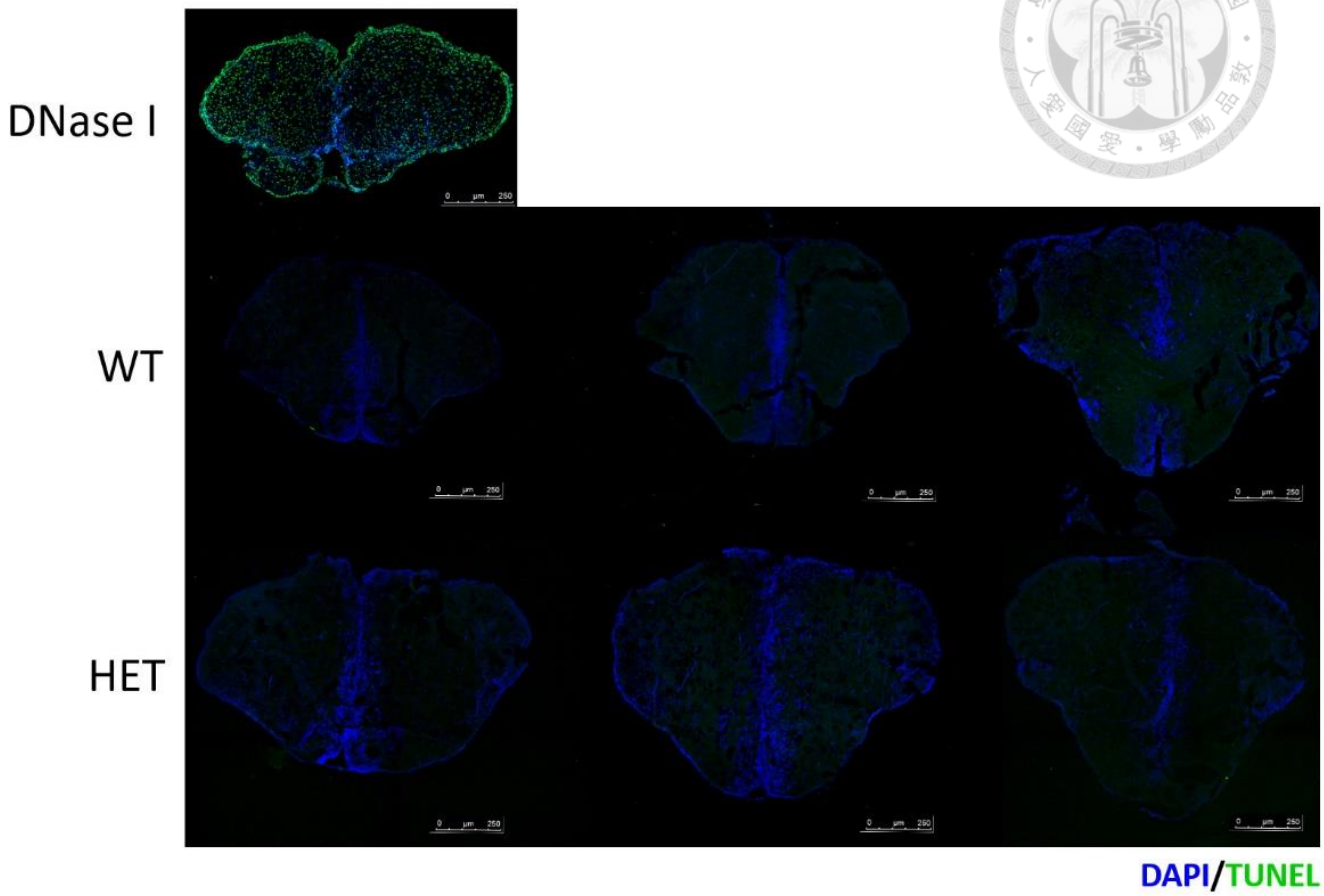

Figure 11. Detection of Apoptosis in Telecephalon of 18 Month *nicastrin*$^{hi1384/+}$ Zebrafish by TUNEL Staining

Plenty of TUNEL signals shown in the positive control (DNase I treated) suggested handling of TUNEL staining procedure was successful. No TUNEL positive signals appeared in telecephalons of both 18 month wild type and *nicastrin*$^{hi1384/+}$ zebrafish.

doi:10.6342/NTU201803306

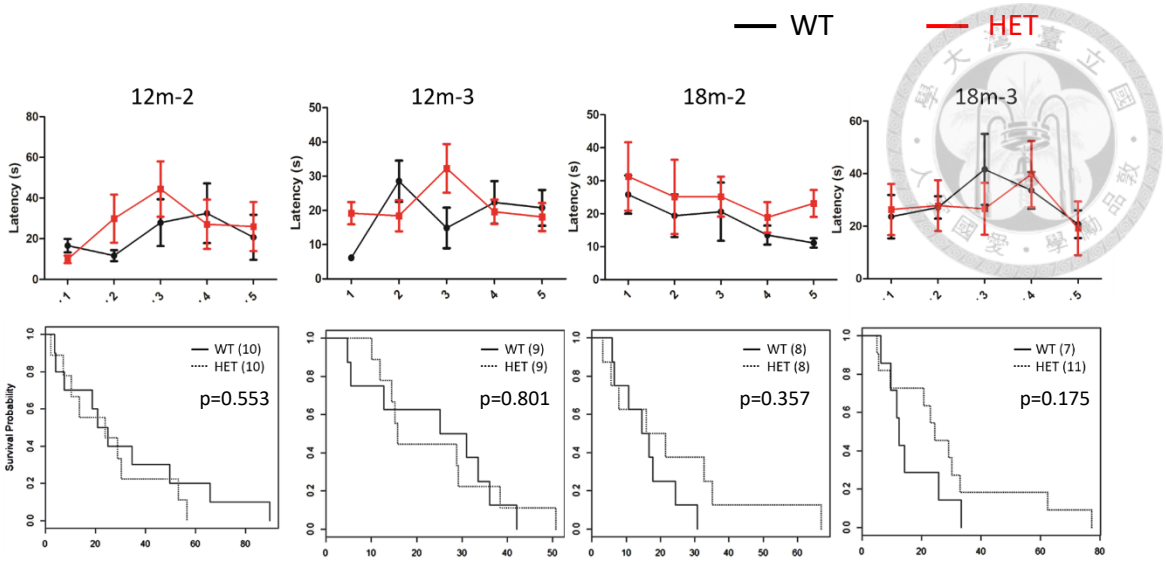

Supplementary Figure 1. Learning Curves of Training Phase and Latency of Test Phase of Latter T-maze Behavioral Tests

As the learning curves showed that finding food latency decreased through last three days in training phase, we considered the subject fish learned where to find the food. No significant difference in the latency of test phase between wild type and *nicastrin*$^{hi1384/+}$ zebrafish in these four experiments. However, 18 month wild type zebrafish reached the food location earlier than 18 month *nicastrin*$^{hi1384/+}$ zebrafish in the test phase.

doi:10.6342/NTU201803306

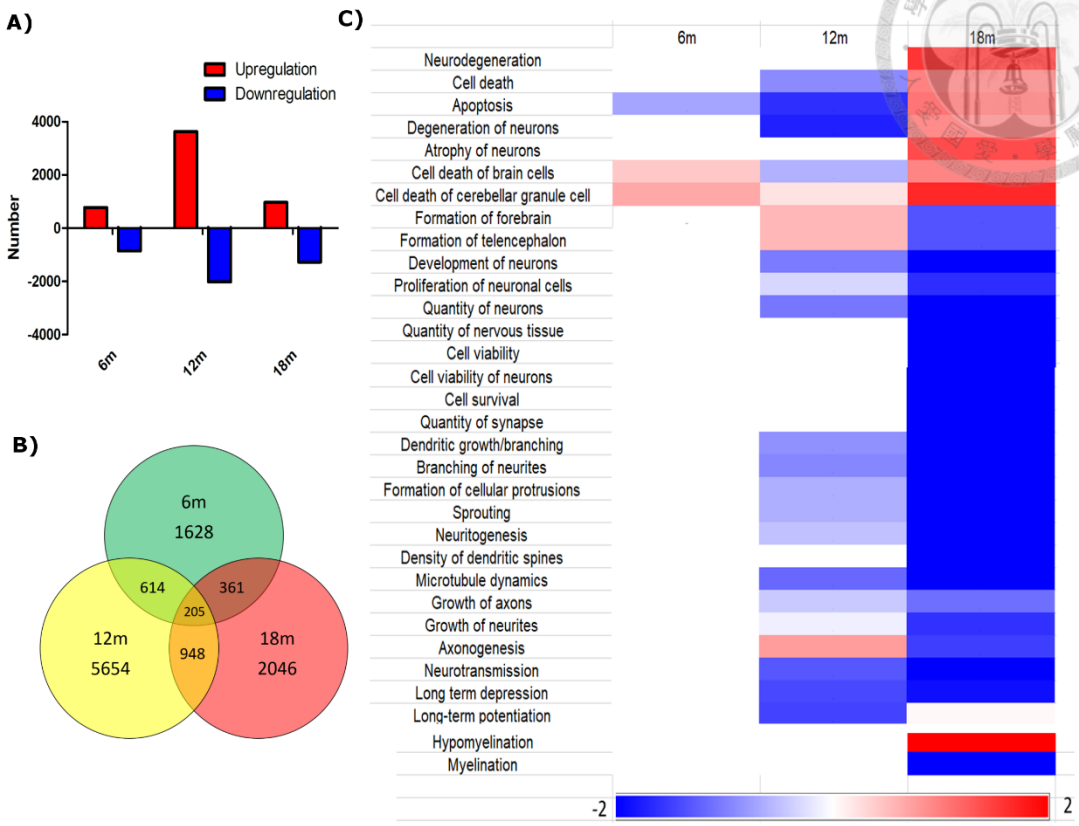

Supplementary Figure 2. Transcriptomic Analysis On Subject Zebrafish of Latter T-maze Behavioral Tests

(A) Overview of Microarray Data. (B) Venn Diagram of Total Number of Affected Genes In The Microarray Data (C) Neurodegeneration were predicted to be activated and neuronal survival and functions were predicted to be inhibited in aged *nicastrin*$^{hi1384/+}$ zebrafish.

doi:10.6342/NTU201803306

Chapter 4. Discussions

4.1 Visual Motor Response of *nicastrin*$^{hi1384/+}$ Zebrafish Larva

In this study, visual motor response test revealed that *nicastrin*$^{hi1384/+}$ zebrafish larva has higher activity but not velocity in the light period. Because wild type and *nicastrin*$^{hi1384/+}$ zebrafish larva can move in the same velocity, the difference in activity might not result from different motor ability, but from slight curling, tingling or whirling implicating the neural circuits of photomotor response were activated at different level between wild type and *nicastrin*$^{hi1384/+}$ larva. As the neural circuits of visual and non-visual dependent photomotor behavior are different (Kokel et al., 2013), it's interesting to study which circuit triggers hyperactivity in *nicastrin*$^{hi1384/+}$ zebrafish larva. Furthermore, we are not sure whether the hyperactivity phenotype would last as *nicastrin*$^{hi1384/+}$ zebrafish grow up. Hyperactivity is related to several psychiatric disorders, such as schizophrenia, attention deficit hyperactivity disorder (ADHD), etc. Actually, it has been demonstrated that *nicastrin* loss of function in oligodendrocytes resulted in hypomyelination in central nervous system and schizophrenia behaviors in mice such as hyperactivity, increased exploratory behavior and repetitive grooming (Dries et al., 2016). Moreover, myelination was predicted to be inhibited and hypomyelination and demyelination was predicted to be activated in aged heterozygous

doi:10.6342/NTU201803306

nicastrin^{hi1384} zebrafish in our microarray data (Supplementary Figure 2). As a result, it's intriguing to examine myelination level and psychiatric disorder phenotypes in adult *nicastrin*$^{hi1384/+}$ zebrafish in the future.

4.2 T-maze Behavioral Tests

4.2.1. Factors That May Lead to Atypical Learning Curve

In the behavioral experiments which are required to train animals, normal subject animals can perform better and better during training sessions. For example, in the T-maze behavioral test, it is expected that subject animals can learn where to find positive rewards and the latency will decrease through serial trainings, or where the negative punishment is and escape from it (Doyle et al., 2017; Lal et al., 2018).

I have to admit that learning curves in the training phase of T-maze behavioral tests in this study were mostly atypical (Figure 5 and Supplementary Figure 1). In my opinion, subject zebrafish tended to quickly find the food cube on the first one or two days of training phase. There are two reasons that can explain this situation in my study. First, we starved the subject for two days before they entered training sessions (Figure 2), so the subject fish suffered hunger and had more desire to look for food on the first day of training phase. As appetite could affect the feeding behavior of zebrafish, it is important

doi:10.6342/NTU201803306

to keep subject zebrafish in a constant unsatieted state in food-based reward behavioral experiments (Gerlai, 2016). Second, we didn't let the subject zebrafish habituate in the T-maze before starting training. As a result, the first day of training phase in this study is the first time for the subject zebrafish to be put in the T-maze. It was likely that the unfamiliarity leaded to anxious behaviors such as hyperactivity. Taken together, we should adjust the scheme of T-maze behavioral test in the future to minimize the influence from other emotions (extreme starvation and anxiety) on the behavior of subject zebrafish.

4.2.2. Age-dependent Memory Decline or Memory Development Failure ?

Original T-maze behavioral test displayed that performance of heterozygous *nicastrin*^{hi1384} zebrafish became significantly worse compared to wild type zebrafish of same age as they grew old (Figure. 6). There are two reasons that can cause the discrepancy. The first one is that *nicastrin*$^{hi1384/+}$ zebrafish suffer from age-dependent memory decline. The other one is that cognitive ability of wild type zebrafish become better as they grow up to 18 months of age and *nicastrin*$^{hi1384/+}$ zebrafish has memory development failure. The latency in the test phase decreased in aged wild type zebrafish compared to the young ones, whereas the latency remained the same in *nicastrin*$^{hi1384/+}$ zebrafish at different age (Figure 6), which suggested that memory development failure leaded to the behavioral discrepancy. However, one can argue that the age-dependent latency decrease of wild type zebrafish might be batch effect as we had difficulty in

doi:10.6342/NTU201803306

maintaining water temperature and the subject zebrafish of different age came from different parents, which could result in different cognitive baseline. From molecular point of view, loss of function of *nicastrin* could impair γ-secretase activity regulation which is involved in both neuronal function and survival. As a result, it's hard to tell which mechanisms or both of them mentioned above resulted in the memory deficits in aged *nicastrin*$^{hi1384/+}$ zebrafish. It's necessary to untangle this problem by carrying out T-maze behavioral test on wild type or *nicastrin*$^{hi1384/+}$ zebrafish of same parent at different age simultaneously in the future.

4.2.3. Reproducibility problem of T-maze behavioral test

As mentioned above, original behavioral test result demonstrated age-dependent memory discrepancy between wild type and *nicastrin*$^{hi1384/+}$ zebrafish. However, we failed to recapitulate the results in the latter experiments (Supplementary Figure 1). Initial result showed the latency of wild type zebrafish in the test phase was significantly shorter than that of *nicastrin*$^{hi1384/+}$ zebrafish at 12 and 18 month of age (Figure 6), whereas latter results showed no significant difference since we had changed the food used in the T-maze behavioral test (Supplementary Figure 1). It has been pointed out that the type of food applied to behavioral test has influence on the experiment results (Manuel et al., 2015; Gerlai, 2016). Nevertheless, 18 month wild type zebrafish still found food more quickly than 18 month *nicastrin*$^{hi1384/+}$ zebrafish in latter T-maze behavioral tests

doi:10.6342/NTU201803306

(Supplementary Figure 1). Furthermore, transcriptomic analysis showed *nicastrin*$^{hi1384/+}$ zebrafish have age-dependent neurodegeneration at transcription level (Figure 7 and Supplementary Figure. 2). Accordingly, we still believe that *nicastrin*$^{hi1384/+}$ zebrafish suffer from age-dependent memory deficits. In the future, we should set up different behavioral platform by using different unconditional stimuli, such as sight of conspecifics, electrical shock or sight of predators to address this problem (Al-Imari and Gerlai, 2008; Xu et al., 2007; Bass and Gerlai, 2008; Gerlai et al., 2009).

4.3 What could we learned from microarray data ?

First, transcriptional analysis by microarray displayed that neurodegeneration associated phenotypes such as apoptosis were predicted to be activated while neurogenesis, neuronal survival and functions were predicted to be inhibited in the aged but not in young *nicastrin*$^{hi1384/+}$ zebrafish's brains (Figure 7 and Supplementary Figure 2), suggesting age-dependent neurodegeneration at transcriptional level appears in *nicastrin*$^{hi1384/+}$ zebrafish. These results are consistent with previous report that loss of *nicastrin* in neurons leads to progressive neurodegeneration, age-dependent memory loss and synaptic dysfunction in mice (Tabuchi et al., 2009; Lee et al., 2014). Furthermore, microarray results in this study indicate that the expression of genes that promote neurodegeneration are upregulated and genes that prevent neurodegeneration are

doi:10.6342/NTU201803306

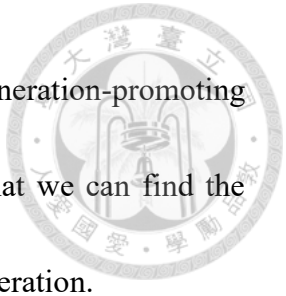

downregulated. Therefore, the next step is to find out those neurodegeneration-promoting or neurodegeneration-preventing genes in the microarray data so that we can find the pathways that lead *nicastrin* deficiency to age-dependent neurodegeneration.

Additionally, microarray results also validated that *nicastrin* mRNA expression was decreased in the brains of *nicastrin*$^{hi1384/+}$ zebrafish, which was further verified by qPCR (Figure 8A and 9A). However, we didn't know if the protein level of Nicastrin also decreased in the brains of *nicastrin*$^{hi1384/+}$ zebrafish. It is known that the four components of γ-secretase can cross-regulate each other coordinately (Steiner et al., 2002; Zhang et al., 2014). Furthermore, it has been reported that *nicastrin* deficiency downregulates the levels of APH-1, Presenilin-1 and PEN-2 and disrupts their intracellular trafficking (Li et al., 2003; Zhang et al., 2005). Therefore, in the future, it's important to examine the protein level of Nicastrin and other γ-secretase subunits in the brains of *nicastrin*$^{hi1384/+}$ zebrafish.

Last, we found gene expression of two genes, *oxt* and *clca1*, which are involved in neurodegeneration are significantly affected in 18 month *nicastrin*$^{hi1384/+}$ zebrafish brains. The mRNA level of *oxt,* which encodes oxytocin is downregulated while that of *clca1* which encodes Calcium-activated Cloride Cannel Regulator was upregulated (Figure. 10). Previous studies displayed that oxytocin could protect neurons from ischemia-induced inflammation, oxidative stress, and excitotoxicity-induced cell death both in vitro and in

doi:10.6342/NTU201803306

vivo (Karelina et al., 2011; Kaneko et al., 2016). Furthermore, it was documented that oxytocin-expressing neurons are significantly decreased in the hypothalamus of Huntington's Disease patients (Gabery et al., 2010). Therefore, downregulation of *oxt* gene expression in 18 month *nicastrin*$^{hi1384/+}$ zebrafish brain could compromise the neuroprotection effect. On the other hand, *clca1* was shown to involve in glutamate-induced excitotoxicity triggered by extrasynaptic NMDA receptors, which could cause cell death (Zhang et al., 2007; Wahl et al., 2009). As a result, upregulation of *clca1* gene in 18 month *nicastrin*$^{hi1384/+}$ zebrafish brain could result in neuronal loss or neuronal dysfunction. However, it's unclear how *nicastrin* downregulation affects the expression of *oxt* and *clca1* gene.

In conclusion, transcriptomic analysis predicted neurodegeneration in aged *nicastrin*$^{hi1384/+}$ zebrafish at transcriptional level, verifying downregulation of *nicastrin* in *nicastrin*$^{hi1384/+}$ zebrafish. Moreover, microarray and qPCR suggested downregulation of *oxt* gene and upregulation of *clca1* gene in 18 month *nicastrin*$^{hi1384/+}$ zebrafish brain. It's interesting to study how *nicastrin* downregulation affects the expression of *oxt* and *clca1* gene and find more candidate molecules from microarray data in the future.

4.4 Potential Neurodegenerative Phenotypes in *nicastrin*$^{hi1384/+}$ Zebrafish

Although transcriptomic analysis predicted *nicastrin*$^{hi1384/+}$ leads to age-dependent

doi:10.6342/NTU201803306

neurodegeneration in zebrafish. However, TUNEL staining showed no significant apoptosis in the telecephlons of *nicastrin*$^{hi1384/+}$ zebrafish at 18 month of age (Figure. 11). Actually, I have conducted TUNEL staining on several telephalon sections from *nicastrin*$^{hi1384/+}$ zebrafish at 3, 6 and 12 month of age and no severe apoptosis detected. A possibility is that it is necrosis but not apoptosis developing in the telecephalon of *nicastrin*$^{hi1384/+}$ zebrafish. However, we don't know whether the number of neurons in the telecephalon of *nicastrin*$^{hi1384/+}$ zebrafish will decrease as they grow old. In addition, neuronal loss might appear at other brain regions, such midbrain or hindbrain. As a result, I think what we can do next is to comprehensively examine neuronal number in the whole brains of aged *nicastrin*$^{hi1384/+}$ zebrafish by conducting immunostaining with neuronal markers such as HuC/D or acetylated tubulin or crossing *nicastrin*$^{hi1384/+}$ zebrafish to zebrafish neuronal reporter lines to examin neuronal loss level in the brains of *nicastrin*$^{hi1384/+}$ zebrafish. On the other hand, It would be interesting to examine if *nicastrin*$^{hi1384/+}$ zebrafish carry other neurodegeneration phenotypes, such as neuroinflammation, and synaptic loss. Additionally, it has been proved that neurodegeneration in zebrafish could induce neurogenesis via an IL4-STAT6 dependent pathway (Bhattarai et al., 2016). One of the feature of zebrafish, which is different from mammals is that zebrafish can regenerate neurons throughout their life. Therefore, it would be intriguing to evaluate the neurogenesis condition in the brains of *nicastrin*$^{hi1384/+}$

doi:10.6342/NTU201803306

zebrafish in the future.

4.5 Comparison of *nicastrin*$^{hi1384/+}$ Zebrafish to Previously Described *nicastrin*-loss-of-function Animal Models

Nicastrin as a subunit of γ-secretase which is involved in many biological pathways and has an intimate relationship in maintaining neuronal survival and function. Loss of *nicastrin* in neurons leads to progressive neurodegeneration in mice which is probably via γ-secretase dependent pathway (Tabuchi et al., 2009; Lee et al., 2014). Moreover, either *presenilin* or *nicastrin* homolog deficiency also causes age-dependent neurodegeneration in *D.melanogaster* as well (Kang et al., 2017), indicating that the role of *nicastrin* in neuronal protection is evolutionarily conserved. Accordingly, there is reason to believe that loss of *nicastrin* in neurons will result in age-dependent neurodegeneration in zebrafish. Consistently, *nicastrin*$^{hi1384/+}$ zebrafish showed potential age-dependent memory deficits and age-dependent neurodegeneration at transcriptional level. However, there are two features where *nicastrin*$^{hi1384/+}$ zebrafish is different from previously mentioned *nicastrin* loss of function flies and mouse models. First, it is highly possible that the expression of *nicastrin* in *nicastrin*$^{hi1384/+}$ zebrafish is downregulated not only in neurons but also in other cells in nervous system, such as astrocytes, microglia/macrophages, oligodendrocytes and even endothelial cells of capillaries in the

doi:10.6342/NTU201803306

brain. The effect of *nicastrin* deficiency on these cells are unclear and it's possible that they work together to contribute to the neurodegeneration phenotypes of *nicastrin*$^{hi1384/+}$ zebrafish we observed so far. For example, depletion of *nicastrin* in oligodendrocytes leads to hypomyelination in central nervous system, which probably happens in the brains of *nicastrin*$^{hi1384/+}$ zebrafish but not in neuronal *nicastrin* conditional knockout mice (Dries et al., 2016) (Figure 7 and Supplementary Figure 2). Second, *nicastrin*$^{hi1384/+}$ zebrafish remain a normal *nicastrin* allele, thus should be considered as a knockdown model rather than a knockout model. We should keep in mind that different phenotypes might occur between knockdown and knockout model of the same gene, which might be attributed to genetic compensation in knockout model (Law and Sargent, 2014; Kok et al., 2015; El-Brolosy and Stainier, 2017). Furthermore, different levels of knockdown also likely to result in different phenotypes. For instance, genetic knockdown of *Psn* (*presenilin* homolog of *D. melnogaster*) in fruit flies via shRNA transgenic lines results in 80%-90% *Psn* mRNA reduction and age-dependent neuronal loss (Kang et al., 2017). On the other hand, heterozygosity of *Psn* only caused age-dependent learning and memory deficits but not neuronal death in fruit flies (McBride et al., 2010). Taken together, I believe that *nicastrin*$^{hi1384/+}$ zebrafish suffer from age-dependent neurodegeneration, and it's possible that the phenotypes of *nicastrin*$^{hi1384/+}$ zebrafish are different from those previously published *nicastrin*-loss-of function animal models and thus could inform us

doi:10.6342/NTU201803306

some associations between *nicastrin* and neurodegenration that could not learn from neuronal conditional *nicastrin* knockout models. However, although this study reveal potential age-dependent memory decline and age-dependent neurodegeneration at transcriptional level in *nicastrin*$^{hi1384/+}$ zebrafish, more solid neurodegeneration phenotypes need to be found in the future so that this model can be applied in neurodegeneration study.

doi:10.6342/NTU201803306

References

Al-Imari, L., Gerlai, R., 2008. Sight of conspecifics as reward in associative learning in zebrafish (Danio rerio). Behavioural Brain Research 189, 216–219.

Amsterdam, A., Nissen, R.M., Sun, Z., Swindell, E.C., Farrington, S., Hopkins, N., 2004. Identification of 315 genes essential for early zebrafish development. Proc Natl Acad Sci U S A 101, 12792-12797.

Babin, P.J., Goizet, C., Raldúa, D., 2014. Zebrafish models of human motor neuron diseases: Advantages and limitations. Progress in Neurobiology 118, 36–58.

Basi, G.S., Hemphill, S., Brigham, E.F., Liao, A., Aubele, D.L., Baker, J., Barbour, R., Bova, M., Chen, X.-H., Dappen, M.S., et al., 2010. Amyloid precursor protein selective gamma-secretase inhibitors for treatment of Alzheimer's disease. Alzheimer's Research & Therapy 2, 36.

Bass, S.L.S., Gerlai, R., 2008. Zebrafish (Danio rerio) responds differentially to stimulus fish: The effects of sympatric and allopatric predators and harmless fish. Behavioural Brain Research 186, 107–117.

Bhattarai, P., Thomas, A.K., Cosacak, M.I., Papadimitriou, C., Mashkaryan, V., Froc, C., Reinhardt, S., Kurth, T., Dahl, A., Zhang, Y., Kizil, C., 2016. IL4/STAT6 Signaling

doi:10.6342/NTU201803306

Activates Neural Stem Cell Proliferation and Neurogenesis upon Amyloid-β42 Aggregation in Adult Zebrafish Brain. Cell Reports 17, 941–948.

Bill, B.R., Petzold, A.M., Clark, K.J., Schimmenti, L.A., Ekker, S.C., 2009. A Primer for Morpholino Use in Zebrafish. Zebrafish 6, 69–77.

Bolduc, D.M., Montagna, D.R., Gu, Y., Selkoe, D.J., Wolfe, M.S., 2016. Nicastrin functions to sterically hinder γ-secretase–substrate interactions driven by substrate transmembrane domain. PNAS 113, E509–E518.

Carroll, C.M., Li, Y.-M., 2016. Physiological and pathological roles of the γ-secretase complex. Brain Res Bull 126, 199–206.

Campbell, W.A., Yang, H., Zetterberg, H., Baulac, S., Sears, J.A., Liu, T., Wong, S.T.C., Zhong, T.P., Xia, W., 2006. Zebrafish lacking Alzheimer presenilin enhancer 2 (Pen-2) demonstrate excessive p53-dependent apoptosis and neuronal loss. Journal of Neurochemistry 96, 1423–1440.

De Strooper, B., Annaert, W., Cupers, P., Saftig, P., Craessaerts, K., Mumm, J.S., Schroeter, E.H., Schrijvers, V., Wolfe, M.S., Ray, W.J., Goate, A., Kopan, R., 1999. A presenilin-1-dependent γ-secretase-like protease mediates release of Notch intracellular domain. Nature 398, 518–522.

doi:10.6342/NTU201803306

De Strooper, B., Iwatsubo, T., Wolfe, M.S., 2012. Presenilins and γ-Secretase: Structure, Function, and Role in Alzheimer Disease. Cold Spring Harb Perspect Med 2, a006304.

De Strooper, B., Karran, E., 2016. The Cellular Phase of Alzheimer's Disease. Cell 164, 603–615.

Doyle, J.M., Merovitch, N., Wyeth, R.C., Stoyek, M.R., Schmidt, M., Wilfart, F., Fine, A., Croll, R.P., 2017. A simple automated system for appetitive conditioning of zebrafish in their home tanks. Behavioural Brain Research 317, 444–452.

Dries, D.R., Zhu, Y., Brooks, M.M., Forero, D.A., Adachi, M., Cenik, B., West, J.M., Han, Y.-H., Yu, C., Arbella, J., Nordin, A., Adolfsson, R., Del-Favero, J., Lu, Q.R., Callaerts, P., Birnbaum, S.G., Yu, G., 2016. Loss of Nicastrin from Oligodendrocytes Results in Hypomyelination and Schizophrenia with Compulsive Behavior. J Biol Chem 291, 11647–11656.

Duggan, S.P., McCarthy, J.V., 2016. Beyond γ-secretase activity: The multifunctional nature of presenilins in cell signalling pathways. Cellular Signalling 28, 1–11.

Dunys, J., Kawarai, T., Sevalle, J., Dolcini, V., George-Hyslop, P.S., Costa, C.A.D., Checler, F., 2007. p53-dependent Aph-1 and Pen-2 Anti-apoptotic Phenotype Requires the Integrity of the γ-Secretase Complex but Is Independent of Its Activity. J. Biol. Chem. 282, 10516–10525.

doi:10.6342/NTU201803306

El-Brolosy, M.A., Stainier, D.Y.R., 2017. Genetic compensation: A phenomenon in search of mechanisms. PLoS Genet 13.

Emran, F., Rihel, J., Dowling, J.E., 2008. A Behavioral Assay to Measure Responsiveness of Zebrafish to Changes in Light Intensities. JoVE (Journal of Visualized Experiments) e923–e923.

Esler, W.P., Kimberly, W.T., Ostaszewski, B.L., Diehl, T.S., Moore, C.L., Tsai, J.-Y., Rahmati, T., Xia, W., Selkoe, D.J., Wolfe, M.S., 2000. Transition-state analogue inhibitors of γ-secretase bind directly to presenilin-1. Nature Cell Biology 2, 428–434.

Gabery, S., Murphy, K., Schultz, K., Loy, C.T., McCusker, E., Kirik, D., Halliday, G., Petersén, A., 2010. Changes in key hypothalamic neuropeptide populations in Huntington disease revealed by neuropathological analyses. Acta Neuropathol. 120, 777–788.

Gerlai, R., 2016. Chapter 17 - Learning and memory in zebrafish (Danio rerio), in: Detrich, H.W., Westerfield, M., Zon, L.I. (Eds.), Methods in Cell Biology, The Zebrafish. Academic Press, pp. 551–586.

Gerlai, R., Fernandes, Y., Pereira, T., 2009. Zebrafish (Danio rerio) responds to the animated image of a predator: Towards the development of an automated aversive task. Behavioural Brain Research 201, 318–324.

doi:10.6342/NTU201803306

Glenner, G.G., Wong, C.W., 1984. Alzheimer's disease: Initial report of the purification and characterization of a novel cerebrovascular amyloid protein. Biochemical and Biophysical Research Communications 120, 885–890.

Golde, T.E., Koo, E.H., Felsenstein, K.M., Osborne, B.A., Miele, L., 2013. γ-Secretase Inhibitors and Modulators. Biochim Biophys Acta 1828.

Goutte, C., Tsunozaki, M., Hale, V.A., Priess, J.R., 2002. APH-1 is a multipass membrane protein essential for the Notch signaling pathway in Caenorhabditis elegans embryos. PNAS 99, 775–779.

Guillozet, A.L., Weintraub, S., Mash, D.C., Mesulam, M.M., 2003. Neurofibrillary Tangles, Amyloid, and Memory in Aging and Mild Cognitive Impairment. Arch Neurol 60, 729–736.

Haass, C., Selkoe, D.J., 1993. Cellular processing of β-amyloid precursor protein and the genesis of amyloid β-peptide. Cell 75, 1039–1042.

Hardy, J.A., Higgins, G.A., 1992. Alzheimer's disease: the amyloid cascade hypothesis. Science 256, 184–185.

Hardy, J., Selkoe, D.J., 2002. The Amyloid Hypothesis of Alzheimer's Disease: Progress and Problems on the Road to Therapeutics. Science 297, 353–356.

Hasegawa, H., Sanjo, N., Chen, F., Gu, Y.-J., Shier, C., Petit, A., Kawarai, T., Katayama, T., Schmidt, S.D., Mathews, P.M., Schmitt-Ulms, G., Fraser, P.E., George-Hyslop,

doi:10.6342/NTU201803306

P.S., 2004. Both the Sequence and Length of the C Terminus of PEN-2 Are Critical for Intermolecular Interactions and Function of Presenilin Complexes. Journal of Biological Chemistry 279, 46455–46463.

Hruscha, A., Krawitz, P., Rechenberg, A., Heinrich, V., Hecht, J., Haass, C., Schmid, B., 2013. Efficient CRISPR/Cas9 genome editing with low off-target effects in zebrafish. Development 140, 4982–4987.

Hsu, C.-H., 2018. Study the roles of two Notch related genes, mind bomb and nicastrin, in zebrafish early development. PhD thesis, National Hsing Hua University, Hsinchu, Taiwan.

Kaneko, Y., Pappas, C., Tajiri, N., Borlongan, C.V., 2016. Oxytocin modulates GABAAR subunits to confer neuroprotection in stroke in vitro. Sci Rep 6.

Kang, J., Shin, S., Perrimon, N., Shen, J., 2017. An Evolutionarily Conserved Role of Presenilin in Neuronal Protection in the Aging Drosophila Brain. Genetics 206, 1479–1493.

Karelina, K., Stuller, K.A., Jarrett, B., Zhang, N., Wells, J., Norman, G.J., DeVries, A.C., 2011. Oxytocin mediates social neuroprotection after cerebral ischemia. Stroke 42, 3606–3611.

doi:10.6342/NTU201803306

Kimberly, W.T., LaVoie, M.J., Ostaszewski, B.L., Ye, W., Wolfe, M.S., Selkoe, D.J., 2003. γ-Secretase is a membrane protein complex comprised of presenilin, nicastrin, aph-1, and pen-2. PNAS 100, 6382–6387.

Kok, F.O., Shin, M., Ni, C.-W., Gupta, A., Grosse, A.S., van Impel, A., Kirchmaier, B.C., Peterson-Maduro, J., Kourkoulis, G., Male, I., DeSantis, D.F., Sheppard-Tindell, S., Ebarasi, L., Betsholtz, C., Schulte-Merker, S., Wolfe, S.A., Lawson, N.D., 2015. Reverse genetic screening reveals poor correlation between Morpholino-induced and mutant phenotypes in zebrafish. Dev Cell 32, 97–108.

Kokel, D., Dunn, T.W., Ahrens, M.B., Alshut, R., Cheung, C.Y.J., Saint-Amant, L., Bruni, G., Mateus, R., Ham, T.J. van, Shiraki, T., Fukada, Y., Kojima, D., Yeh, J.-R.J., Mikut, R., Lintig, J. von, Engert, F., Peterson, R.T., 2013. Identification of Nonvisual Photomotor Response Cells in the Vertebrate Hindbrain. J. Neurosci. 33, 3834–3843.

Kumar, A., Singh, A., Ekavali, 2015. A review on Alzheimer's disease pathophysiology and its management: an update. Pharmacological Reports 67, 195–203.

Lal, P., Tanabe, H., Suster, M.L., Ailani, D., Kotani, Y., Muto, A., Itoh, M., Iwasaki, M., Wada, H., Yaksi, E., Kawakami, K., 2018. Identification of a neuronal population in the telencephalon essential for fear conditioning in zebrafish. BMC Biol 16, 45.

doi:10.6342/NTU201803306

Law, S.H.W., Sargent, T.D., 2014. The Serine-Threonine Protein Kinase PAK4 Is Dispensable in Zebrafish: Identification of a Morpholino-Generated Pseudophenotype. PLOS ONE 9, e100268.

Lee, S.-F., Shah, S., Yu, C., Wigley, W.C., Li, H., Lim, M., Pedersen, K., Han, W., Thomas, P., Lundkvist, J., Hao, Y.-H., Yu, G., 2004. A Conserved GXXXG Motif in APH-1 Is Critical for Assembly and Activity of the γ-Secretase Complex. J. Biol. Chem. 279, 4144–4152.

Lee, S.H., Sharma, M., Südhof, T.C., Shen, J., 2014. Synaptic function of nicastrin in hippocampal neurons. PNAS 111, 8973–8978.

Li, J., Fici, G.J., Mao, C.-A., Myers, R.L., Shuang, R., Donoho, G.P., Pauley, A.M., Himes, C.S., Qin, W., Kola, I., Merchant, K.M., Nye, J.S., 2003. Positive and Negative Regulation of the γ-Secretase Activity by Nicastrin in a Murine Model. J. Biol. Chem. 278, 33445–33449.

Lim, A., Moussavi Nik, S.H., Ebrahimie, E., Lardelli, M., 2015. Analysis of nicastrin gene phylogeny and expression in zebrafish. Dev. Genes Evol. 225, 171–178.

Manuel, R., Zethof, J., Flik, G., Bos, R. van den, 2015. Providing a food reward reduces inhibitory avoidance learning in zebrafish. Behavioural Processes 120, 69–72.

Martín-Jiménez, R., Campanella, M., Russell, C., 2015. New Zebrafish Models of Neurodegeneration. Curr Neurol Neurosci Rep 15, 33.

doi:10.6342/NTU201803306

Masters, C.L., Simms, G., Weinman, N.A., Multhaup, G., McDonald, B.L., Beyreuther, K., 1985. Amyloid plaque core protein in Alzheimer disease and Down syndrome. PNAS 82, 4245–4249.

McBride, S.M.J., Choi, C.H., Schoenfeld, B.P., Bell, A.J., Liebelt, D.A., Ferreiro, D., Choi, R.J., Hinchey, P., Kollaros, M., Terlizzi, A.M., Ferrick, N.J., Koenigsberg, E., Rudominer, R.L., Sumida, A., Chiorean, S., Siwicki, K.K., Nguyen, H.T., Fortini, M.E., McDonald, T.V., Jongens, T.A., 2010. Pharmacological and genetic reversal of age dependent cognitive deficits due to decreased presenilin function. J Neurosci 30, 9510–9522.

Mitani, Y., Yarimizu, J., Saita, K., Uchino, H., Akashiba, H., Shitaka, Y., Ni, K., Matsuoka, N., 2012. Differential Effects between γ-Secretase Inhibitors and Modulators on Cognitive Function in Amyloid Precursor Protein-Transgenic and Nontransgenic Mice. J. Neurosci. 32, 2037–2050.

Newman, M., Ebrahimie, E., Lardelli, M., 2014. Using the zebrafish model for Alzheimer's disease research. Front Genet 5.

Ochalek, A., Mihalik, B., Avci, H.X., Chandrasekaran, A., Téglási, A., Bock, I., Giudice, M.L., Táncos, Z., Molnár, K., László, L., Nielsen, J.E., Holst, B., Freude, K., Hyttel, P., Kobolák, J., Dinnyés, A., 2017. Neurons derived from sporadic Alzheimer's

doi:10.6342/NTU201803306

disease iPSCs reveal elevated TAU hyperphosphorylation, increased amyloid levels, and GSK3B activation. Alzheimer's Research & Therapy 9.

Osmundson, T.W., Eyre, C.A., Hayden, K.M., Dhillon, J., Garbelotto, M.M., 2013. Back to basics: an evaluation of NaOH and alternative rapid DNA extraction protocols for DNA barcoding, genotyping, and disease diagnostics from fungal and oomycete samples. Molecular Ecology Resources 13, 66–74.

Paquet, D., Bhat, R., Sydow, A., Mandelkow, E.-M., Berg, S., Hellberg, S., Fälting, J., Distel, M., Köster, R.W., Schmid, B., Haass, C., 2009. A zebrafish model of tauopathy allows in vivo imaging of neuronal cell death and drug evaluation. J Clin Invest 119, 1382–1395.

Pardossi‐Piquard, R., Dunys, J., Giaime, E., Guillot‐Sestier, M.-V., George‐Hyslop, P.S., Checler, F., Costa, C.A. da, 2009. p53-Dependent control of cell death by nicastrin: lack of requirement for presenilin-dependent γ-secretase complex. Journal of Neurochemistry 109, 225–237.

Plant, L.D., Boyle, J.P., Smith, I.F., Peers, C., Pearson, H.A., 2003. The Production of Amyloid β Peptide Is a Critical Requirement for the Viability of Central Neurons. J. Neurosci. 23, 5531–5535.

Prince, M.J., 2016. World Alzheimer Report 2016 - Improving healthcare for people living with dementia: Coverage, quality and costs now and in the future.

doi:10.6342/NTU201803306

Schmid, B., Haass, C., 2013. Genomic editing opens new avenues for zebrafish as a model for neurodegeneration. Journal of Neurochemistry 127, 461–470.

Sesele Katia, Thanopoulou Kalliopi, Paouri Evi, Tsefou Eliona, Klinakis Apostolos, Georgopoulos Spiros, 2013. Conditional inactivation of nicastrin restricts amyloid deposition in an Alzheimer's disease mouse model. Aging Cell 12, 1032–1040.

Shih, I.-M., Wang, T.-L., 2007. Notch Signaling, γ-Secretase Inhibitors, and Cancer Therapy. Cancer Res 67, 1879–1882.

Steiner, H., Winkler, E., Edbauer, D., Prokop, S., Basset, G., Yamasaki, A., Kostka, M., Haass, C., 2002. PEN-2 Is an Integral Component of the γ-Secretase Complex Required for Coordinated Expression of Presenilin and Nicastrin. J. Biol. Chem. 277, 39062–39065.

Tabuchi, K., Chen, G., Südhof, T.C., Shen, J., 2009. Conditional Forebrain Inactivation of Nicastrin Causes Progressive Memory Impairment and Age-Related Neurodegeneration. J. Neurosci. 29, 7290–7301.

Thinakaran, G., Parent, A.T., 2004. Identification of the role of presenilins beyond Alzheimer's disease. Pharmacological Research, Alzheimer disease 50, 411–418.

Tanyeri, G., Celik, O., Erbas, O., Oltulu, F., Yilmaz Dilsiz, O., 2015. The effectiveness of different neuroprotective agents in facial nerve injury: An experimental study. Laryngoscope 125, E356-364.

doi:10.6342/NTU201803306

Urban, S., 2016. Nicastrin guards Alzheimer's gate. PNAS 113, 1112–1114.

Vetrivel, K.S., Zhang, Y., Xu, H., Thinakaran, G., 2006. Pathological and physiological functions of presenilins. Molecular Neurodegeneration 1, 4.

Wahl, A.-S., Buchthal, B., Rode, F., Bomholt, S.F., Freitag, H.E., Hardingham, G.E., Rønn, L.C.B., Bading, H., 2009. Hypoxic/ischemic conditions induce expression of the putative pro-death gene Clca1 via activation of extrasynaptic N-methyl-d-aspartate receptors. Neuroscience, Protein trafficking, targeting, and interaction at the glutamate synapse 158, 344–352.

Wang, Y., Mandelkow, E., 2016. Tau in physiology and pathology. Nature Reviews Neuroscience 17, 22–35.

Wolfe, M.S., Xia, W., Ostaszewski, B.L., Diehl, T.S., Kimberly, W.T., Selkoe, D.J., 1999. Two transmembrane aspartates in presenilin-1 required for presenilin endoproteolysis and γ-secretase activity. Nature 398, 513–517.

Xi, Y., Noble, S., Ekker, M., 2011. Modeling Neurodegeneration in Zebrafish. Curr Neurol Neurosci Rep 11, 274–282.

Xie, T., Yan, C., Zhou, R., Zhao, Y., Sun, L., Yang, G., Lu, P., Ma, D., Shi, Y., 2014. Crystal structure of the γ-secretase component nicastrin. PNAS 111, 13349–13354.

Xu, X., Scott-Scheiern, T., Kempker, L., Simons, K., 2007. Active avoidance conditioning in zebrafish (Danio rerio). Neurobiology of Learning and Memory 87, 72–77.

doi:10.6342/NTU201803306

Zhang, Y., Luo, W., Wang, H., Lin, P., Vetrivel, K.S., Liao, F., Li, F., Wong, P.C., Farquhar, M.G., Thinakaran, G., Xu, H., 2005. Nicastrin Is Critical for Stability and Trafficking but Not Association of Other Presenilin/γ-Secretase Components. J. Biol. Chem. 280, 17020–17026.

Zhang, X., Li, Y., Xu, H., Zhang, Y., 2014. The γ-secretase complex: from structure to function. Front Cell Neurosci 8.

Zhang, S.-J., Steijaert, M.N., Lau, D., Schütz, G., Delucinge-Vivier, C., Descombes, P., Bading, H., 2007. Decoding NMDA Receptor Signaling: Identification of Genomic Programs Specifying Neuronal Survival and Death. Neuron 53, 549–562.

Zhao, G., Liu, Z., Ilagan, M.X.G., Kopan, R., 2010. γ-Secretase Composed of PS1/Pen2/Aph1a Can Cleave Notch and Amyloid Precursor Protein in the Absence of Nicastrin. J. Neurosci. 30, 1648–1656.

Zhao, Y., Li, X., Huang, T., Jiang, L.-L., Tan, Z., Zhang, M., Cheng, I.H.-J., Wang, X., Bu, G., Zhang, Y.-W., Wang, Q., Xu, H., 2017. Intracellular trafficking of TREM2 is regulated by presenilin 1. Exp. Mol. Med. 49, e405.

doi:10.6342/NTU201803306

Appendix. Antibody Test for Zebrafish Endogenous Tau Protein

Appendix-1 Material Methods

Appendix 1-1 Western Blot

Dissected zebrafish brains were lysed with RIPA buffer (150 mM NaCl, 50 mM Tris-HCl pH.8, 1% Triton X-100, 0.5% sodium deoxycholate, 50 mM β-glycerophosphate, 1 mM Na_3VO_4 and protease inhibitor 1:500) and quantified by BCA assay. After quantification, 1/5 volume of sample buffer was added, boiled at 98°C to denature proteins. 30-50 μg of proteins were loaded and polyacrylamide gel electrophoresis (PAGE) was conducted with 70 mV to separate proteins. Separated proteins in the polyacrylamide gel were transferred to PVDF membrane at 4°C with 60 mV for 2.5 hours or 20 mV overnight. Proteins on the PVDF membrane were washed with TBST, blocked in blocking buffer (2% BSA in TBST) for 1 hr at RT or 4°C overnight. Then the PVDF membranes were stained with primary antibody for 2 hours at RT or 4°C overnight, washed with TBST for 10 minutes for 3 times, then stained with corresponding secondary antibody for an hour at RT. Finally the membranes were washed with TBST for 3 times in an hour and treated with ECL to develop luminescence. Images were acquired in the Advanced Imaging System (UVP Biospectrum 500).

doi:10.6342/NTU201803306

Appendix 1-2 Mass Spectrometry

Peptides samples for mass spectrometry were prepared according to the standard protocol provided from NHRI Core Facility for Proteomics and Chemistry. In short, Zebrafish brain proteins lysates were acquired as mentioned. Targeted zebrafish Tau protein candidate was immunoprecipitated by GTX129892 primary antibody and then boiled in sample buffer at 98 °C for 5 minutes. The immunoprecipated lysate was separated by PAGE (Figure A2. B). GTX129892-immunoprecipitated proteins which were predicted zebrafish Tau proteins in the polyacrylamide gel were stained with silver nitrate, cut down and destained in destaining working solution (15 mM $K_3[Fe(CN)_6]$, 50 mM $Na_2S_2O_3$), and then 20 mM NH_4HCO_3. Next, acetonitrile was added for dehydration. After acetonitrile was dried up in a CVE-3100 Centrifugal Evaporator (Eyela, Tokyo, Japan), the disulfide bonds of proteins were removed by reduction in reduction solution (10 mM dithiothreitol, 10 mM NH_4HCO_3) at 56 °C for 15 minutes and then alkylation in alkylation solution (55 mM Iodoacetamide, 10 mM NH_4HCO_3) in the dark at room temperature for 20 minutes. Then the proteins in the gel were washed with 10 mM NH_4HCO_3 / 50 % acetonitrile and dehydrated in acetonitrile. After dry up of acetonitrile, the proteins in the gel were treated with enzyme solution (10 ng/μL trypsin, 10 mM NH_4HCO_3) at 4 °C. After the gel became transparent, 10 mM NH_4HCO_3 was added and

doi:10.6342/NTU201803306

incubated at 37 °C overnight to digest the proteins into peptides. Later, the supernatant was transferred to a new Eppendorf vial. To acquire as more peptides as possible, twice peptides extraction procedures were carried out where the gel was treated with 50% acetonitrile / 1% formic acid and sonicated for 10 minutes, and then the supernatant was pooled with the former extracted peptides. Afterwards, the peptides were dried up overnight. Next, 0.1% formic acid was added to dissolve peptides, and Zip-Tip was used to remove remaining ions. Finally, the peptides were eluted with 10 μL elution solution (75% acetonitrile, 1 % formic acid). Afterwards, the peptides sample was delivered to and Mass Spectrometry (NanoUPLC-ESI-MS/MS) was conducted in the NHRI Core Facility for Proteomics and Chemitry.

Appendix 1-3 Plasmid and mRNA Generation

First, zebrafish brain cDNA library was acquired as mentioned. The *maptb* cDNA were PCR-amplified with a pair of primers (Forward: GGGCCCCTCGAGATGGACCATCAGGACCACATG; Reversse: GGGCCCTCTAGATCACAGGCCTTGTTTAGCAAGG) designed according to NCBI database (XM_009299377). Then, the *maptb* cDNA fragments were subcloned into pCS2+MT vectors at XhoI and XbaI sites (pCS2-MT-Maptb) (Figure A1). The sequence was verified by DNA sequencing which was done by NHRI DNA sequencing Core Lab.

doi:10.6342/NTU201803306

Next the *myc-maptb* mRNA were synthesized following the instruction of mMASSAGE mMACHINE Sp6 Transcription Kit (Thermo).

Appendix 1-4 HEK293T cells Transfection

HEK293T cells were seeded in 9 mm^2 culture dishes at a density of 10^5 cells per dish in 3 mL Dulbecco's modified Eagles medium (DMEM) medium (Life Technology, 11995-040) supplemented with 10% FBS (GIBCO, 10437028) in 9 mm^2 culture dish in an incubator at 37°C with 5% CO_2 for 24 hours to reach about 60% confluence befor transfection. Afterwards, transfection was performed with Lipofectamine™ 3000 Transfection Kit (Invitrogen, L3000-001). Specifically, HEK293T cells were cultured in with serum free medium, and 2 μg plasmid DNA and 10 μL Lipofectamine™ 3000 Reagent was used for each dish and incubated for 2 hours. Then the medium was replaced with serum-containing medium and incubated for 24 hours. After 24 hours incubation, transfected cells were ready for western blot experiments mentioned above.

Appendix 1-5 Zebrafish Embryo Microinjection

For microinjection, the injection needles were made by a micropipette puller (MODEL P-97) with a fixed setup (heat 60, pull 180, vel 150, del 100, p 500, ramp 587). 120 ng of *myc-maptb* mRNA were injected into each zebrafish embryo. 24 hours after

doi:10.6342/NTU201803306

injection, 50 *myc-maptb* mRNA injected zebrafish embryos and control embryos (No injection) were collected and the chorions were removed in 10 mg/mL pronase. The yolk was removed by deyolking buffer (55 mM NaCl, 1.8 mM KCl, 1.25 mM $NaHCO_3$) and washed with deyolking wash buffer (110 mM NaCl, 3.5 mM KCl, 2.7 mM $CaCl_2$, 10 mM Tris-HCl pH8.5). Afterwards the embryos were ready for subsequent western blot procedure mentioned above.

Appendix 1-2. Results and Discussions

As Tau proteins in aged heterozygous *nicastrin*^{hi1384} zebrafish brain were hyperphosphorylated in our preliminary study (unpublished data). Accordingly, it's intriguing to find out when the Tau proteins in the heterozygous *nicastrin*^{hi1384} zebrafish brains start to be hyperphosphorylated. However, the antibody which had been used to detect zebrafish endogenous Tau proteins was depleted and not available anymore. Therefore, I managed to seek antibodies that can detect zebrafish endogenous Tau proteins from several Tau antibodies developed to target human or mouse Tau (Table A1). Initially, there were two antibodies from GeneTex, which are GTX129892 and GTX130456, showed signals in zebrafish brain western blot (Figure A2.A). GTX129892 was developed to target human Tau proteins phosphorylated at Ser400, while GTX130456 was generated to target human Tau proteins phosphorylated at Ser198. The western blot

doi:10.6342/NTU201803306

signals derived from GTX129892 appeared at 70 kDa position (Figure A2.A), whereas the signal derived from GTX130456 located at 55 kDa (Figure A2.A). Database on NCBI shows zebrafish might carry both high molecular and low molecular weight Tau proteins, indicating these two kinds of antibodies might detect different zebrafish Tau proteins. However, we didn't know whether these signals were truly derived from zebrafish endogenous Tau proteins. For further examination, mass spectrometry was carried out on GTX129892 purified proteins by immunoprecipitation (Figure A2.B). It turned out that the protein which was bound by GTX129892 antibody was most likely to be DPYL3 (Dihydropyrimidase Like 3) (Table A2), but not zebrafish endogenous Tau proteins. On the other hand, as there is difficulty to purify GTX130456-detected proteins, I managed to overexpress zebrafish endogenous Tau proteins with six Myc tag on the C-terminal (Figure A1) in HEK293T cells and zebrafish embryos, and examined whether GTX130456 antibody could detect the overexpressed zebrafish endogenous Tau proteins by western blot. GTX130456 antibody failed to detect overexpressed Myc-tagged zebrafish Tau proteins in both HEK293T cells (Figure A2.C) and zebrafish embryos (Figure A2.D). These results indicated that both GTX129892 and GTX130456 could not detect zebrafish endogenous Tau proteins. As Tau proteins hyperphosphorylation is a significant feature in many neurodegenerative diseases, it's necessary to find out when Tau proteins in the brains of *nicastrin*$^{hi1384/+}$ zebrafish start to be hyperphosphorylated.

doi:10.6342/NTU201803306

Therefore, we should develop antibodies that can specifically bind zebrafish endogenous Tau proteins by ourselves, as it seems that all the commercial antibodies targeting human Tau proteins cannot bind zebrafish endogenous Tau proteins.

doi:10.6342/NTU201803306

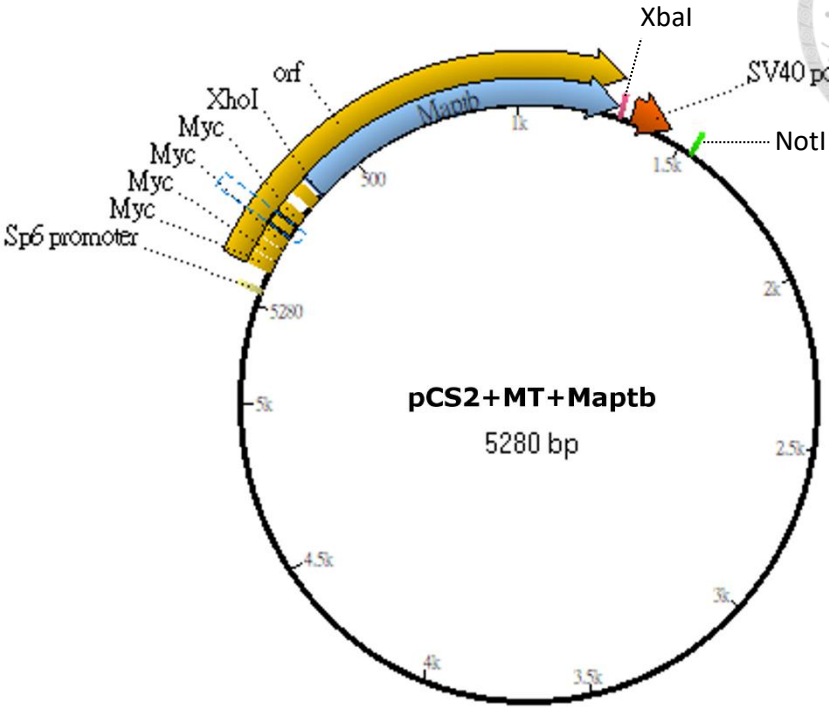

Figure A1. The construction of pCS2-MT-Maptb plasmid

Maptb was inserted into pCS2 at 3'end of Myc tag between XhoI and XbaI restriction enzyme cutting site.

doi:10.6342/NTU201803306

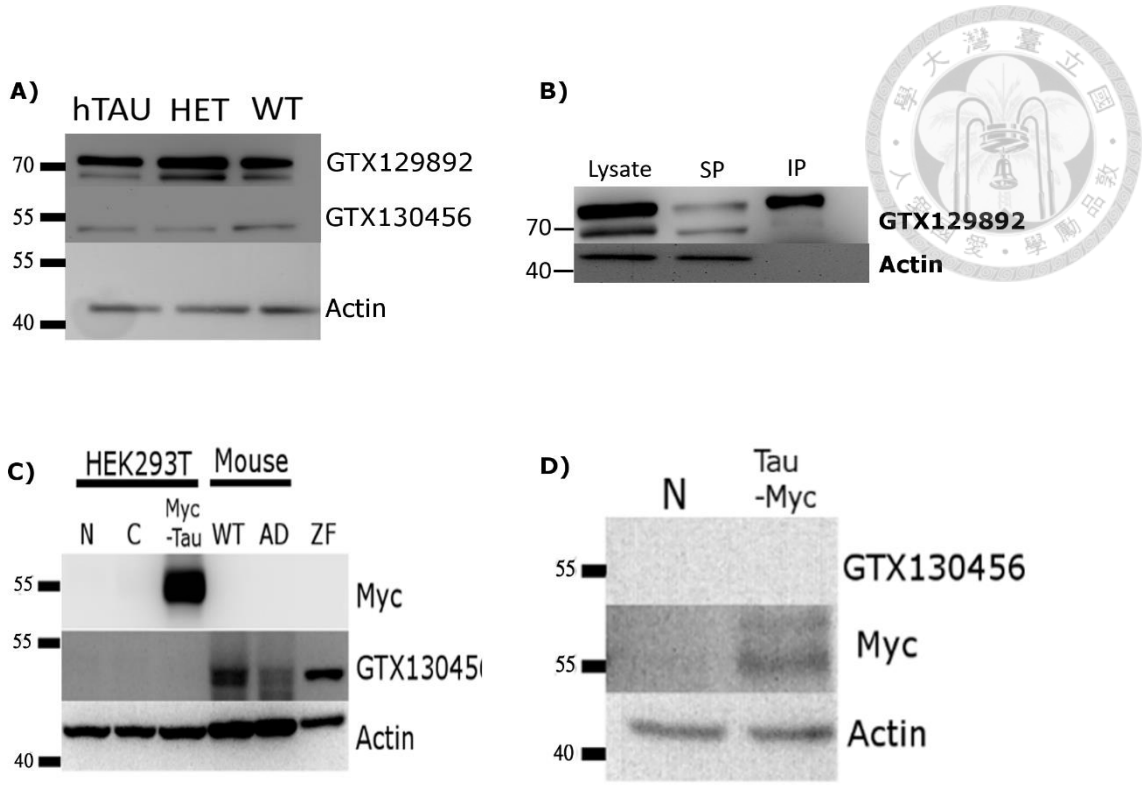

Figure A2. Test of Human Tau Antibody on Zebrafish Tau Proteins

(A) Among the tested human Tau antibodies, only GTX129892 and GTX130456 had signals near 70 kDa and 50 kDa respectively. (hTAU represents mde3; mde4 zebrafish which can generate human Tau proteins under the control of HuC promoter (Paquet et al., 2009)); HET: *nicastrin*$^{hi1384/+}$) (B) Immunoprecipitation with GTX129892 Antibody and Western Blot By The Same Antibody In The Following. (SP: Supernatant; IP: Immunoprecipitated proteins) (C) Western blot on HEK293T cells transfected with C (pCS2+MT) or Myc-Tau plasmids (pCS2+MT+Maptb) or not transfected HEK293T cells. Mouse brain lysates from wild type or Alzheimer's disease mouse model were used as positive control. ZF: zebrafish. Myc-tagged

doi:10.6342/NTU201803306

zebrafish endogenous Tau proteins overexpressed in HEK293T cells (C) or zebrafish embryos (D) couldn't be detected by GTX130456 antibody.

Table A1 List of Tested Tau Antibodies

Antibody Names	Source	Target	Reactivity	Concentration	Signal
GTX112981	Genetex	pan-tau	Human, Rat	1:1000	X
GTX129892	Genetex	p400 tau	Human, Mouse	1:2000	V
GTX130456	Genetex	p198 tau	Human, Mouse, Rat	1:2000	V
GTX130462	Genetex	pan-tau	Mouse	1:1000	X
GTX116044	Genetex	pan-tau	Human	1:1000	X
GTX100866	Genetex	pan-tau	Human, Mouse	1:2000	X

Table A2 The Protein Matched to Peptides Hit in Mass Spectrometry

Accession	Symbol	Score	Mass	Peptide score	Peptide sequence
NP_001018348.1	Dihydropyrimidase related protein 3 (DPYSL3)	100	61904	52.29	SAADIISQAR
				68.93	GTTTADDFTQGTK
				43.01	AVTIASQTNCPLYVTR

doi:10.6342/NTU201803306

List of Abbreviations

%	percentage degree
WT	wild type zebrafish
HET	heterozygous *nicastrin*^{hi1384} zebrafish
nicastrin$^{hi1384/+}$	heterozygous *nicastrin*^{hi1384}
dpf	Days post fertilization
M	molar
mM	millimolar
μL	microliter
μg	microgram
H&E staining	hematoxylin and eosin staining
TUNEL	Terminal deoxynucleotidyl transferase dUTP nick end labeling
PCR	polymerase chain reaction
DNA	deoxyribonucleic acid
RNA	ribonucleic acid
PBS	phosphate buffered saline
PFA	paraformaldehyde
EDTA	ethylenediaminetetraacetic acid
qPCR	quantitative real-time PCR
cDNA	complementary deoxyribonucleic acid
bp	base pair
mRNA	messenger ribonucleic acid
rps24	Ribosome Protein S24
clca1	Calcium-activated Chloride Channel Regulator

doi:10.6342/NTU201803306